

# **Analysis of Dissimilar Metal Welding of 1020 Mild Steel and 304 Stainless Steel**

**Tayyab Islam**



**Department of Mechanical Engineering  
National Institute of Technology  
Rourkela – 769008**

# **Analysis of Dissimilar Metal Welding of 1020 Mild Steel and 304 Stainless Steel**

A Thesis Submitted in  
The Partial Fulfilment of the Requirements for the degree of

**Master of Technology**  
In  
**Production Engineering**

By  
**Tayyab Islam**  
(Roll No: 211ME2171)

Under the Supervision of  
**Dr. S.K. Sahoo**



**Department of Mechanical Engineering**  
**National Institute of Technology**  
**Rourkela – 769008**



**National Institute of Technology**  
**Rourkela- 769008** [www.nitrkl.ac.in](http://www.nitrkl.ac.in)

**Dr. S.K. Sahoo**  
Professor  
Department of Mechanical Engineering

### **CERTIFICATE**

This is to certify that the thesis entitled **Analysis of Dissimilar Metal Welding of 1020 Mild Steel and 304 Stainless Steel** submitted by **Tayyab Islam** (211ME2171) in the partial fulfilment of the requirements for the degree of **Master of Technology** in Production Engineering is an authentic work carried out by him under my supervision and guidance. To the best of my knowledge, the matter embodied in this thesis has not been submitted elsewhere for the award of any degree or diploma.

**Dr. S.K. Sahoo**

**Date:** 30<sup>th</sup> of May 2014

**Place:** Rourkela

## **Acknowledgements**

First of all I would like to thank Almighty Allah for the successful completion of this project. Indeed I have toiled and worked hard for this project but its completion is only through the grace of Almighty.

I would like to express my sincere gratitude to my guide Dr. S.K. Sahoo for providing me an opportunity to work with him and his continuous assistance throughout the course of this research project. His constant advice, appreciation and assessment have been very vital to provide the constant thrust to go on and complete this work. He has been the pillar of strength for me during this project work.

I would also like to thank Prof. K.P. Maity Head of the Department, Mechanical Engineering for providing me and all my colleagues' excellent departmental infrastructure during our entire degree program. I am also obliged to my faculty advisor Dr. S.K. Patel for guiding us throughout the curriculum and providing us vital inputs and information from the administration.

At last I thank my parents who gave me an upbringing to have the opportunity to study in such a prestigious institute.

**Tayyab Islam**

**Date:** 30<sup>th</sup> of May 2014

**Place:** Rourkela

## **Abstract**

Joining of dissimilar metals has found its use extensively in power generation, electronic, nuclear reactors, petrochemical and chemical industries mainly to get tailor-made properties in a component and reduction in weight. However efficient welding of dissimilar metals has posed a major challenge due to difference in thermo-mechanical and chemical properties of the materials to be joined under a common welding condition.

This causes a steep gradient of the thermo-mechanical properties along the weld. A variety of problems come up in dissimilar welding like cracking, large weld residual stresses, migration of atoms during welding causing stress concentration on one side of the weld, compressive and tensile thermal stresses, stress corrosion cracking, etc.

Weld residual stress and thermal stress have been analysed for dissimilar metal welding of 304 stainless steel to 1020 mild steel taking 302 stainless steel as the filler metal. Similarly taking strain developed as an index the susceptibility of the welded joint to stress corrosion cracking have been studied. It is found that when the filler metal is replaced by Inconel 625 significant improvement is obtained in the welded joint in terms of reduction in stress developed and stress corrosion cracking.

Also the problem of carbon migration is eliminated by the use of Inconel 625 as a weld filler metal due to the resistance of nickel-based alloys to any carbon diffusion through them.

**Keywords-** dissimilar welding; stress corrosion cracking; thermal stress; residual stress.

## **List of Figures**

<b>Fig. No.</b>	<b>Title of the Figure</b>	<b>Page No.</b>
Fig. 1.	Types of Welded Joints	2
Fig. 2.	Zones in a Welding Joint	3
Fig. 3.	Stress in welds (a) thermal stress during & (b) residual stress after welding	5
Fig. 4.	Factors influencing Stress Corrosion Cracking	6
Fig. 5.	Schematic representation of the welded joint	20
	Case I: 302 Stainless Steel as weld filler metal	
Fig. 6.	Normal stress contour of Model A	22
Fig. 7.	Normal stress distribution along line P	23
Fig. 8.	Shear stress contour of Model A	23
Fig. 9.	Shear stress distribution along line P	24
Fig. 10.	Normal stress contour of Model B	24
Fig. 11.	Normal stress distribution along line P	25
Fig. 12.	Shear stress contour of Model B	25
Fig. 13.	Shear stress distribution along line P	26
Fig. 14.	Normal stress contour of Model C	26
Fig. 15.	Normal stress distribution along line P	27
Fig. 16.	Shear stress contour of Model C	27
Fig. 17.	Shear stress distribution along line P	28
Fig. 18.	Equivalent strain contour in Model C	28
Fig. 19.	Equivalent strain distribution along line P	29
	Case I: Inconel 625 as weld filler metal	
Fig. 20.	Normal stress contour of Model A	29
Fig. 21.	Normal stress distribution along line P	30

Fig. 22.	Shear stress contour of Model A	30
Fig. 23.	Shear stress distribution along line P	31
Fig. 24.	Normal stress contour of Model B	31
Fig. 25.	Normal stress distribution along line P	32
Fig. 26.	Shear stress contour of Model B	32
Fig. 27.	Shear stress distribution along line P	33
Fig. 28.	Normal stress contour of Model C	33
Fig. 29.	Normal stress distribution along line P	34
Fig. 30.	Shear stress contour of Model C	34
Fig. 31.	Shear stress distribution along line P	35
Fig. 32.	Equivalent strain contour in Model C	35
Fig. 33.	Equivalent strain distribution along line P	36
Fig. 34.	Comparison of strain values between case I and case II	38

## **List of Tables**

<b>Table No.</b>	<b>Title of the Figure</b>	<b>Page No.</b>
Table 1.	Composition of 304 Stainless Steel	15
Table 2.	Composition of 1020 Mild Steel	15
Table 3.	Composition of Inconel 625	15
Table 4.	Mechanical Properties of 304 Stainless Steel	16
Table 5.	Mechanical Properties of 1020 Mild Steel	16
Table 6.	Mechanical Properties of Inconel 625	17
Table 7.	Thermal Properties of 304 Stainless Steel	18
Table 8.	Thermal Properties of 1020 Mild Steel	18
Table 9.	Thermal Properties of Inconel 625	19
Table 10.	Comparison of normal stress values in the two cases of welding	36



## **Table of Contents**

<b>Certificate</b>	ii
<b>Acknowledgements</b>	iii
<b>Abstract</b>	iv
<b>List of figures</b>	v
<b>List of tables</b>	vii
<b>1. Introduction</b>	1
1.1. History	1
1.2. Weld Processes	1
1.2.1. Fusion Welding	2
1.2.2. Forge Welding	2
1.3. Welded Joints	2
1.4. Metallurgy of a Welded Joint	3
1.5. Dissimilar Welding	4
1.6. Stresses for Welded Joints	4
1.6.1. Residual Stress	4
1.6.2. Thermal Stress	5
1.6.3. Thermal Stress superimposed under Residual Stress	6
1.7. Stress Corrosion Cracking (SCC)	6
1.8. Carbon Migration	7
1.9. Aim of the Research	8
<b>2. Literature Survey</b>	9
2.1. Research Papers	9
2.2. Summary	13

<b>3.</b>	<b>Problem Formulation</b>	14
<b>3.1.</b>	<b>Input Parameters</b>	14
3.1.1.	Composition	14
3.1.2.	Mechanical Properties	15
3.1.3.	Thermal Properties	17
<b>3.2.</b>	<b>Finite Element Analysis</b>	19
<b>3.3.</b>	<b>Problem Statement</b>	20
<b>3.4.</b>	<b>Assumptions and Conditions</b>	21
<b>4.</b>	<b>Results and Discussion</b>	22
<b>4.1.</b>	<b>Case 1: 302 Stainless Steel as Weld Filler Metal</b>	22
<b>4.2.</b>	<b>Case 2: Inconel 625 as Weld Filler Metal</b>	29
<b>5.</b>	<b>Conclusions</b>	39
<b>6.</b>	<b>References</b>	40

# Chapter 1

## Introduction

Welding is a manufacturing process of creating a permanent joint obtained by the fusion of the surface of the parts to be joined together, with or without the application of pressure and a filler material. The materials to be joined may be similar or dissimilar to each other. The heat required for the fusion of the material may be obtained by burning of gas or by an electric arc. The latter method is more extensively used because of greater welding speed.

Welding is extensively used in fabrication as an alternative method for casting or forging and as a replacement for bolted and riveted joints. It is also used as a repair medium e.g. to reunite a metal at a crack or to build up a small part that has broken off such as a gear tooth or to repair a worn surface such as a bearing surface.

### 1.1. History

Welding, a metal joining process can be traced back in history to the ancient times. In the Bronze Age, nearly 2000 years ago, circular boxes made of gold were welded in lap joint arrangement by applying pressure. Later on in the Iron Age, Egyptians started welding pieces of iron together. But welding as we know nowadays came into existence only in the 19<sup>th</sup> century.

Sir Humphrey Davy produced an electric arc using two carbon electrodes powered by a battery. This principle was subsequently applied to weld metals. Resistance welding finally developed in the year 1885 by Elihu Thomson. Acetylene gas was discovered in 1836 by Edmund Davy, but it could not be used in welding application due to lack of a proper welding torch. When the require welding torch was invented in 1900, oxy-acetylene welding became one of the most popular type of welding mainly due to its relatively lower cost. However in the 20<sup>th</sup> century it lost its place to arc welding in most of the industrial applications.

Advance welding techniques like Plasma Arc Welding, Laser Beam Welding, Electron Beam Welding, Electro-Magnetic Pulse Welding, Ultrasonic Welding, etc. are now being extensively used in electronic and high precision industrial applications.

### 1.2. Weld Processes

The welding processes may be broadly classified into the following two groups:

1. Welding processes that use heat alone i.e. Fusion Welding.
2. Welding processes that use a combination of heat and pressure i.e. Forge Welding.

### 1.2.1. Fusion Welding

In case of fusion welding the parts to be joined are held in position while the molten metal is supplied to the joint. The molten metal may come from the parts themselves i.e. parent metal or filler metal which normally has the same or nearly similar composition as that of the parent metal. Thus, when the molten metal solidifies or fuses, the joint is formed. The fusion welding, according to the method of heat generated, may be classified as:

1. Thermite Welding
2. Gas Welding
3. Electric Arc Welding

### 1.2.2. Forge Welding

In forge welding, the parts to be joined are first heated to a proper temperature in a furnace and then hammered. Electric Resistance Welding is an example of forge welding. The principle of applying heat and pressure, either sequentially or simultaneously is widely used in the processes known as Spot, Seam, Projection, Upset and Flash Welding.

## 1.3. Welded Joints

The welding joint geometry can be classified primarily into five types. This is based on the orientation between the material surfaces to be joined. The various joints are shown in the figure 1 below:

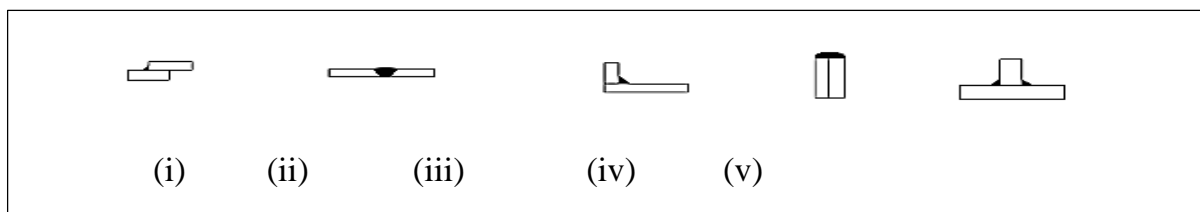


Fig 1: *Types of Welded Joints*

- (i) Lap Joint
- (ii) Butt Joint
- (iii) Corner Joint
- (iv) Edge Joint
- (v) T-Joint

The main considerations involved in the selection of a particular welded joint are given below:

1. The shape of the welded component required,
2. The thickness of the plates to be welded, and
3. The direction of the forces to which the finished object will be subjected to in the actual working conditions.

## 1.4. Metallurgy of a Welded Joint

Metal is heated over the range of temperature up to fusion and followed by cooling ambient temperature. Due to differential heating, the material away from the weld bead will be hot but as the weld bead is approached progressively higher temperatures are obtained, resulting in a complex micro structure. The subsequent heating and cooling results in setting up internal stresses and plastic strain in the weld.

Depending upon the slope of temperature gradient three distinct zones as shown in Fig. 2 can be identified in welded joint which are:

1. Base metal
2. Heat Affected Zone (HAZ)
3. Weld metal

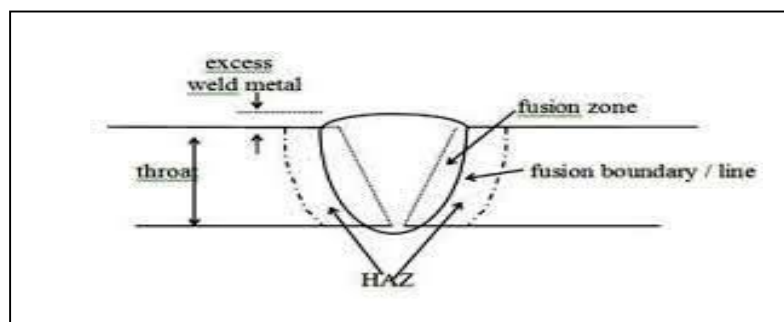


Fig 2: Zones in a welding joint

A joint produced without a filler metal is called autogenous and its weld zone is composed of re-solidified base metal. A joint made with a filler metal is called weld metal. Since central portion of the weld bead will be cooled slowly, long columnar grains will developed and in the out ward direction grains will become finer and finer with distance.

So the ductility and toughness decreases away from the weld bead. However strength increases with the distance from the weld bead. The original structure in steels consisting of ferrite and pearlite is changed to alpha iron. The weld metal in the molten state has a good tendency to dissolve gases which come into contact with it like oxygen, nitrogen and hydrogen.

So during solidification, a portion of these gases get trapped into the bead called porosity. Porosity is responsible for decrease in the strength of the weld joint. Cooling rates can be controlled by preheating of the base metal welding interface before welding.

The heat affected zone is within the base metal itself. It has a microstructure different from that of the base metal after welding, because it is subjected to elevated temperature for a substantial period of time during welding. In the heat affected zone, the heat applied during welding recrystallizes the elongated grains of the base metal, grains that are away from the weld metal will recrystallizes into fine equiaxed grains.

## **1.5. Dissimilar Welding**

Joining of dissimilar metals has found its use extensively in power generation, electronic, nuclear reactors, petrochemical and chemical industries mainly to get tailor-made properties in a component and reduction in weight. However efficient welding of dissimilar metals has posed a major challenge due to difference in thermo-mechanical and chemical properties of the materials to be joined under a common welding condition. This causes a steep gradient of the thermo-mechanical properties along the weld.

A variety of problems come up in dissimilar welding like cracking, large weld residual stresses, migration of atoms during welding causing stress concentration on one side of the weld, compressive and tensile thermal stresses, stress corrosion cracking, etc. Now before discussing these problems coming up during dissimilar welding, the passages coming below throw some light on some of the causes of these problems.

In dissimilar welds, weldability is determined by crystal structure, atomic diameter and compositional solubility of the parent metals in the solid and liquid states. Diffusion in the weld pool often results in the formation of intermetallic phases, the majority of which are hard and brittle and are thus detrimental to the mechanical strength and ductility of the joint.

The thermal expansion coefficient and thermal conductivity of the materials being joined are different, which causes large misfit strains and consequently the residual stresses results in cracking during solidification.

## **1.6. Stresses for Welded Joints**

The stresses in welded joints are difficult to determine because of the variable and unpredictable parameters like homogeneity of the weld metal, thermal stresses in the welds, changes in physical properties due to high rate of cooling, etc. In design problems, these stresses are obtained on the following assumptions:

1. The load is distributed uniformly along the entire length of the weld, and
2. The stress is spread uniformly over its effective section.

### **1.6.1. Residual Stress**

Residual stress is a tension or compression that exists in a material without any external load being applied, and the residual stresses in a component or structure are caused by incompatible internal permanent strains. Welding, which is one of the most significant cause of residual stress, typically produces large tensile stresses, the maximum value of which is approximately equal to the yield strength of materials that are joined by lower compressive residual stresses in a component. The residual stress of welding can significantly impair the performance and reliability of welded structures.

Two of the major problems of any welding process are residual stress and distortion. Residual stress is primarily caused by the compressive yielding that occurs around the molten zone as the material heats and expands during welding. When the weld metal cools it contracts which causes a tensile residual stress, particularly in the longitudinal direction.

After welding a residual tensile stress remains across the weld centreline and causes a balancing compressive stress further from the weld zone. The tensile residual stress on the weld line reduces the fatigue strength and the toughness, particularly when combined with any notches or defects associated with the weld bead.

To relieve some of the residual stresses caused by the welding process, the structure deforms, causing distortion. There are several modes of distortion, but the one that is most common, particularly in thin welded structures is buckling distortion, which is caused by the compressive stress in the parent material. The residual stress developed after welding is shown in Fig 3 (b).

### 1.6.2. Thermal Stresses

In dissimilar metal welding, one of the metals in contact at the weld metal interface is constrained by expansion or contraction of the other. The two metals being welded possess different coefficient of thermal expansion. The metal having a higher coefficient of thermal expansion, with its tendency to expand more than the other is constrained by the fixed boundary.

As a result of which compressive thermal stress is developed in the metal having a higher coefficient of thermal expansion while tensile thermal stress is developed in the metal with the lower coefficient of thermal expansion. The thermal stress developed during the welding is shown in Fig 3 (a).

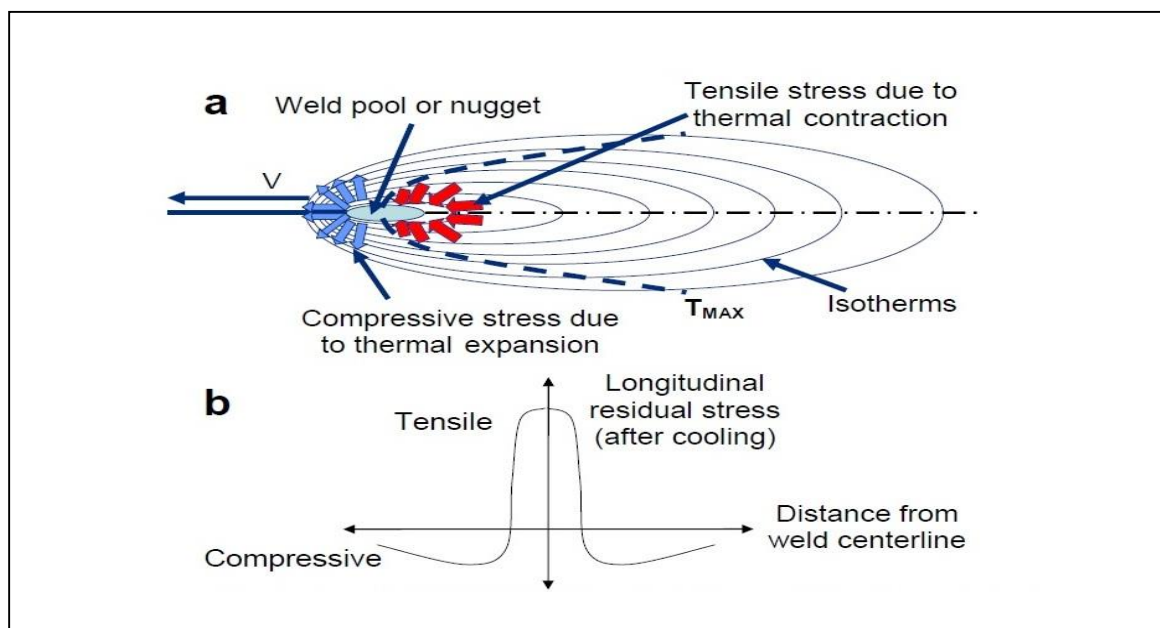


Figure 3: Stress in welds (a) thermal stress during & (b) residual stress after welding.

### 1.6.3. Thermal Stress Superimposed under Residual Stress

The welded metal parts are subjected to a numerous cycles of thermal expansion and contraction. As result of which these thermal stresses get superimposed over the residual stress induced after welding.

A correct estimate of thermal stresses under superimposed condition with the residual stress is necessary to determine the weakest zone or the area most susceptible to cracking. The cyclic thermal stresses superimpose on the weld residual stress and operating tensile stresses can promote brittle fracture, increase the susceptibility of a weld to fatigue damage and stress corrosion cracking (SCC) during service. This will ensure a sound design of the joint and structural integrity.

### 1.7. Stress Corrosion Cracking (SCC)

Stress corrosion cracking is cracking due to a process involving conjoint corrosion and straining of a metal due to residual or applied stresses. The impact of SCC on a material usually falls between dry cracking and the fatigue threshold of that material. SCC usually occurs in certain specific alloy-environment-stress combinations. SCC is a corrosion mechanism that requires the pairing of a material with a very particular environment and the application of a tensile stress above a critical value.

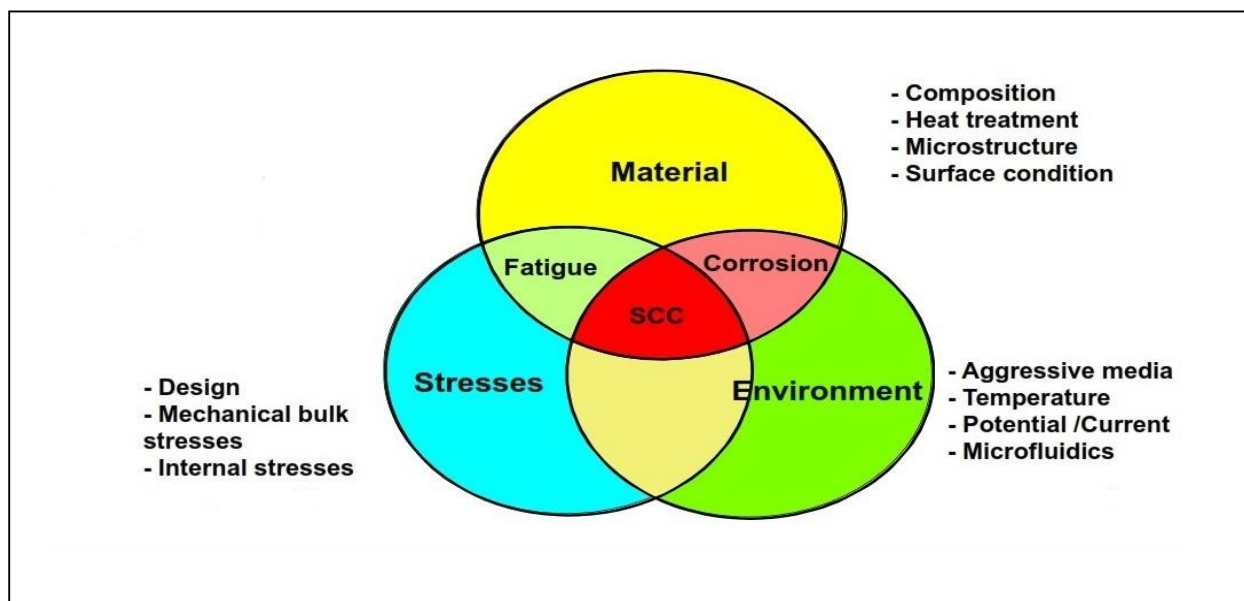


Fig 4: Factors influencing Stress Corrosion Cracking

As shown in Fig. 4 above Stress Corrosion Cracking is not just a material problem, but it is a combined result of the following three factors:

1. Material Properties
2. Corrosive Environment
3. Stresses



Most of the surface is not attacked, but with fine cracks penetrating into the material. In the microstructure, these cracks can have an intra-granular or a trans-granular morphology. Macroscopically, SCC fractures have a brittle appearance. SCC is classified as a catastrophic form of corrosion, as the detection of such fine cracks can be very difficult and the damage not easily predicted. Typical SCC failures are seen in pressure vessels, pipework, stressed components and systems where an excursion from normal operating conditions or the environment occurs.

Stress Corrosion Cracking can be controlled by the incorporating the measures given below:

1. Selecting a material that is not susceptible to the service environment
2. Ensuring that any changes to the environment caused by cleaning are not detrimental to the material.
3. Controlling the service stresses through careful design and minimising stress concentrations to keep them below the critical value.
4. Heat Treatment reduces the residual stresses in the material and in turn decreases the susceptibility to Stress Corrosion Cracking.
5. Using corrosion inhibitors during cleaning operations or to control the environment in a closed system.
6. Coating the material and effectively isolating the material from the environment.

## **1.8. Carbon Migration**

Carbon migration across the weld interface is considered a significant factor in the "life" of a transition joint, since time dependent property changes occur in the regions where carbon movement occurs.

The carbon migration causes loss of strength in the ferrite material adjacent to the weld interface and an increase in hardness (and probably also in strength with a change in the modulus of elasticity possible) in the filler metal (carbon-enriched zone). These zones are immediately adjacent to one another and provide a significant change in properties across a narrow region.

However, some generalizations can be stated concerning carbon migration in a welded joint:

1. Carbon migration is directly dependent on time, temperature and carbon content of the base metals.
2. Carbon diffuses five to ten times faster in ferrite than in austenite at the same temperature.
3. Thermal stresses acting on the weld interface enhance carbon diffusion, thus the metals having larger co-efficient of thermal expansion like stainless steel will experience more rapid formation of the carbon depleted zone.

4. The carbon depleted zone exhibits low tensile and creep strength and reduced recrystallization temperature. However, the properties are not specifically defined.
5. The carbon-depleted soft zone is restrained by the harder and stronger carbon-enriched zone immediately adjacent during thermal cycling. The development of a complex stress state involving shear along the interface, thus inhibiting uniform strain and tends to create deformations in the soft zone.

### **1.9. Aim the research**

The aim of the present work is to simulate a welding joint between 304 stainless steel and 1020 mild steel using 302 stainless steel as the weld metal and analyse the joint for thermal and residual stresses developed in them. Then the weld joint is to be analysed for residual stresses superimposed on thermal stresses.

After the results are obtained the aim is to suggest improvement in the joint by minimizing the stresses and reducing chances of stress corrosion cracking by a change in the weld metal.

## Chapter 2

### Literature Survey

Over the years a lot of research has been done in the area of dissimilar welding and many interesting results have been brought up with regards to the problems encountered in dissimilar welding. With dissimilar welding finding its use in nuclear, petrochemical, electronics and several other industrial domains, this section brings into account the work of the predecessors in this field.

#### 2.1. Research papers

Chengwu et al. [1] in their work on weld interface microstructure and mechanical properties of copper-steel dissimilar welding, the microstructure near the interface between Cu plate and the intermixing zone was investigated. Experimental results showed that for the welded joint with high dilution ratio of copper, there was a transition zone with numerous filler particles near the interface.

However, if the dilution ratio of copper is low, the transition zone is only generated near the upper side of the interface. [1] At the lower side of the interface, the turbulent bursting behaviour in the welding pool led to the penetration of liquid metal into Cu. The welded joint with lower dilution ratio of copper in the fusion zone exhibited higher tensile strength.

Jiang and Guan [2] studied the thermal stress and residual stress in dissimilar steels. They suggested that large residual stresses are induced by welding in the weld metal and heat affected zone (HAZ), which superimpose and increase the thermal stress.

Gyun Na, Kim and Lim [3] studied the residual stress and its prediction for dissimilar welds at nuclear plants using Fuzzy Neural network models. The factors that have an impact upon fatigue strength are residual stress, stress concentration, the mechanical properties of the material, and its micro and macro structure.

Gyun Na et al. [3] stated that residual stress is one of the most important factors but its effect on high-cycle fatigue is of more concern than the other factors. Residual stress is a tension or compression that exists in a material without any external load being applied, and the residual stresses in a component or structure are caused by incompatible internal permanent strains.

Welding, which is one of the most significant causes of residual stress, typically produces large tensile stresses, the maximum value of which is approximately equal to the yield strength of materials that are joined by lower compressive residual stresses in a component. [3] The residual stress of welding can significantly impair the performance and reliability of welded structures. The integrity

of welded joints must be ensured against fatigue or corrosion during their long use in welded components or structures.

On stress corrosion cracking Gyun Na et al. [3] stated that stress-corrosion cracking usually occurs when the following three factors exist at the same time: susceptible material, corrosive environment, and tensile stress including residual stress. Thus, residual stress becomes very critical for stress-corrosion cracking when it is difficult to improve the material corrosiveness of the components and their environment under operating conditions.

Khan et al. [4] studied laser beam welding of dissimilar stainless steels in a fillet joint configuration and during the study metallurgical analysis of the weld interface was done. Fusion zone microstructures contained a variety of complex austenite ferrite structures. Local micro-hardness of fusion zone was greater than that of both base metals.

The welding fusion zone microstructure consists of mostly primary ferrite dendrites with an inter-dendritic layer of austenite. [4] This austenite forms through a peritectic–eutectic reaction and exists at the ferrite solidification boundaries at the end of solidification. Some lathy ferrite morphology is also observed in this zone. This is due to restricted diffusion during ferrite–austenite transformation that results in a residual ferrite pattern.

Khan et al. [4] came to the conclusion that formation of ferrite along the austenite grain boundary in the heat affected zone on austenite side is observed. At the same time, microstructures are composed of two-phase ferrite and martensite with intra-granular carbide on ferrite side. Also the variation in local micro-hardness observed across the weld depends on the fraction intermix of each base metal and the redistribution of austenite- and ferrite-promoting elements in the weld.

Itoh et al. [5] got a patent on the joined structure on the dissimilar metallic materials. This invention relates generally to a joined structure of dissimilar metallic materials having different characteristics. More specifically, the invention relates to a joined structure of a current carrying contact or arching contact which are used for, e.g., a power breaker, or a coating end structure of a metal base and a coating material for improving conductivity and heat resistance.

Delphin, Sattari-Far and Brickstad [6] studied the effect of thermal and weld residual stresses on CTOD (Crack Tip Opening Displacement) in elastic-plastic fracture analysis. They stated that structures may fail because of crack growth both in welds and in the heat affected zone (HAZ). The welding process itself induces residual stresses in the weld and HAZ, which contribute to crack growth.

Delphin et al. [6] used a non-linear thermoplastic finite element model to simulate the circumferential weld in a relatively thin-walled stainless steel pipe. After the pipe had cooled down after welding a circumferential surface crack was introduced. The crack, located in the centre of the weld, was subjected to two types of

loads. Firstly, the welded pipe was subjected to a primary tensile load, and then to a secondary thermal load.

Delphin et al. [6] stated that the choice of hardening model is important. It is believed that kinematic hardening is a better choice than isotropic hardening in low cycle simulations i.e. in a few-pass welding process, as in the present study.

For the case of weld residual stresses in combination with high thermal stresses, it is found that the plasticity induced by the thermal stresses is not sufficient to suppress the influence of weld residual stresses on CTOD, even for very high thermal loads. The residual stresses can be relaxed by unloading from a primary tensile load.

Mai and Spowage [7] did their work on characterisation of dissimilar joints of steel-kovar, copper-steel and aluminium-copper. It was stated in their work that joining of dissimilar materials is one of the challenging tasks facing modern manufacturers.

Dissimilar metal welding technologies find application in many sectors such as micro-electronics, medical, optoelectronics and microsystems. [7] The tiny geometry of the joints and the different optical and thermal properties of the materials makes laser welding one of the most suitable production methods.

Also high temperature gradients in a welding may result in martensitic reactions leading to excessive hardness in the fusion zone. [7] The X-ray stress analysis technique was unable to resolve the stress variations generated by the different processing parameters used. In similar steel welds the residual stress at the centre of the weld pool has been reported to be close to the material yield strength.

Colegrove et al. [8] studied the welding process impact on residual stress and distortion. Their work seeks to understand the relationship between heat input, fusion area, measured distortion and the residual stress predicted from a simple numerical model, and the residual stresses is validated with experimental data.

Residual stress is caused by the compressive yielding that is occurring around the molten zone when the material is heated and its expansion during welding. [8] When the weld metal cools it gets contracted which results to a tensile residual stress, primarily in the longitudinal direction.

After the welding is over, a residual tensile stress is present across the weld centreline which causes a balancing compressive stress away from the weld zone. [8] The tensile residual stress on the weld centreline decreases the fatigue strength and toughness, especially when combined with any of the notches or other defects related to the weld bead.

The other main finding of Colgrove et al. [8] is that the heat input and distortion go with each other in nearly a linear relationship. The results obtained for the residual stress show that the width of the peak tensile increases with heat input. Finally the residual stress measurements indicate how the tensile peak widens up with

increasing the heat input. There is a very small difference in the magnitude of the peak tensile for the different welding processes.

Arunkumar, Duraisamy and Manikandan [9] studied the mechanical properties of dissimilar metal tube welded joints and named some of the alloying elements that improve the weldability of the welded joint. Alloy Steels such as that contain chromium and molybdenum. This composition delivers good weldability and high hardenability for the above stated alloys.

Chromium provides improved oxidation and corrosion resistance. And molybdenum increases strength at elevated temperature. [9] The combination of chromium and molybdenum also increases resistance to high temperature hydrogen attack and to creep.

Arunkumar et al. [9] also stated that excessive penetration of a weld root can be rectified by proper alignment of tubes in root of weld joint; concentric bore at ends, correct welding current. Porosity in welded joint can be reduced by using low hydrogen welding process, increasing shielding gas flow, increasing heat input and using clean joint faces.

Chung et al. [10] studied microstructure and stress corrosion cracking behaviour of the weld metal in dissimilar welds and susceptibility to stress corrosion cracking in terms of ductility loss is dependent in increasing order of severity is; undiluted weld metal, the transition zone and the weld interface. This means that susceptibility to stress corrosion cracking is more related to the case of brittle fractures.

Chung et al. [10] stated that interface cracking is often associated with a hardened interface region in the weld, implying that the weld interface plays an important role in determining SCC susceptibility.

Chung et al. [10] also observed that the microstructures near the weld interface are complicated, consisting of martensite and carbides. Apparently, their presence caused inter-granular cracking and significantly reduced the SCC resistance of the weld. Additionally, the structural discontinuity at the interface also increases the SCC susceptibility of the weld interface specimen.

One of the very important inferences from the study of Chung et al. [10] was that the presence of alloying elements in the heat affected zone and fusion zone varied with distance from the weld interface, as a result, the SCC susceptibility changed accordingly. The more Ni and Cr contents, the less the specimen would be susceptible to SCC.

Lundin [11] did his research on dissimilar welds with its emphasis on carbon migration, stress/strain state of welds and transition joint failure mechanism. The study stated that the majority of failures have been associated with austenitic stainless steel filler metal joints, and it is considered that the failure mode exhibited by the

nickel-based filler metals is fundamentally different than that with the austenitic stainless fillers.

Lundin [11] said that the cracking most often initiates at or near the outside surface. The cracking results directly from void linkup, grain boundary separation or tearing. It is generally parallel to the weld interface. The cracking is associated with or exacerbated by oxidation- oxide notching. The relative expansion coefficients of the various weld metal regions are extremely important with regard to thermal stress generation.

Increasing the Ni content of the filler metal alters carbon solubility, makes carbides less stable, changes diffusivity and in general retards carbon migration from the ferritic material. [11] The influence of time, temperature and material composition influences the nickel rich weld metals reduces carbon migration. Further, the use of stabilizing elements in the ferritic component is effective in combatting migration but neither so easily employed nor ultimately effective for long time exposure.

## **2.2. Summary**

To summarize the literature studied it must be said that the stresses developed in dissimilar welding are very different from these in similar welding. Residual stress present in the weld metal and HAZ of parent metals makes the part very susceptible to stress corrosion cracking. The residual stress, if not considered while designing the welded joint leads to an underestimation of the actual stresses and ultimately the part fails in its stated service life.

The literature also confirms that nickel based alloys exhibit a better tensile strength, resistance to carbon activity and lower strain hardening than stainless steels. So a nickel based alloy is more suitable to be used as weld filler metal for welding steels.

## Chapter 3

### Problem Formulation

The aim of this research project has been to study dissimilar metal joint using a filler metal. Dissimilar welding is used to fabricate the pressure vessels and piping in power plant but failures occur frequently due to:

1. Thermal Stress which is generated due to difference in co-efficient of thermal expansion.
2. Difference in mechanical properties, the local heating and subsequent cooling results in large residual stress.

This thermal stress superimposed on weld residual stress and operating tensile stress promotes brittle fracture, increase susceptibility to fatigue and stress corrosion cracking during its service life. The domain of this research covers cause, effect and elimination of problems caused due to stresses, carbon migration and stress corrosion cracking.

The metals to be welded are 304 stainless steel and 1020 plain carbon steel and the filler metal used is 302 Stainless steel whose properties has been taken similar to 304 stainless steel for the purpose of analysis.

The welding process has been simulated using finite element analysis. The software used for this analysis is ANSYS 13.0 using its Workbench module. It is because Workbench is a very powerful tool to simulate a welding joint and infer the results. Also it has a reputation of coming up with results very close to the practical values. The input parameters are easily fed and boundary conditions, simulation programmes and geometrical modelling is very convenient due to its user-friendly graphic interface.

### 3.1. Input Parameters

The input parameters in this analysis are the thermo-mechanical properties of the materials getting into the welding joint. All the properties used in this analysis are temperature dependent.

#### 3.1.1. Composition

The composition of the metals used in this simulation of welding joint is given below:

##### 1. 304 Stainless Steel

The composition of 304 stainless steel is shown in table 1. Chromium along with nickel is the principal alloying elements.



Table 1: *Composition of 304 Stainless Steel*

<b>Fe</b>	<b>C</b>	<b>Si</b>	<b>Mn</b>	<b>S</b>	<b>P</b>	<b>Cr</b>	<b>Ni</b>
71.433	0.058	0.35	1.32	0.007	0.032	18.52	8.28

## 2. 1020 Mild Steel

In plain carbon steel, carbon is the principle alloying element. Composition of 1020 mild steel is shown in table 2.

Table 2: *Composition of 1020 Mild Steel*

<b>Fe</b>	<b>C</b>	<b>Mn</b>	<b>P</b>	<b>S</b>
99.31	0.2	0.4	0.04	0.05

## 3. 302 Stainless Steel

The composition of 302 stainless steel is almost similar to that of 304 stainless steel and the composition has been taken same for the purpose of analysis. 302 stainless steel has been used as the weld metal in the first analysis and subsequently replaced by Inconel 625 in the second analysis.

## 4. Inconel 625

Inconel 625 is a non-magnetic, corrosion and oxidation resistant, nickel-based alloy. This alloy has high fatigue strength, exhibits excellent resistance to stress corrosion cracking. Nickel and Chromium provide stabilizing effect from oxidizing environments. The nickel based alloys like Inconel also resist problems caused due to carbon migration.

Pitting and crevice corrosion are prevented by Molybdenum stabilizes the alloy against sensitization during welding. Due to these properties, Inconel is widely used in dissimilar welding. The composition of Inconel 625 which has been used in this analysis has been shown in Table 3.

Table 3: *Composition of Inconel 625*

<b>Ni</b>	<b>Cr</b>	<b>Mo</b>	<b>Fe</b>	<b>Mn</b>	<b>C</b>	<b>Cu</b>	<b>Si</b>
61.5	23.0	8.0	6.5	0.25	0.08	0.2	0.25

### 3.1.2. Mechanical Properties

The mechanical properties that have been chosen for the purpose of analysis are density, Poisson's ratio, modulus of elasticity and yield strength. The mechanical and thermal properties of the materials used in this analysis have been extrapolated

from the graph published by Jiang and Guan [2] in their study on residual stress in a welded joint.

### 1. 304 Stainless Steel

The mechanical properties of 304 stainless steel that have been used in this analysis have been given in table 4.

Table 4: *Mechanical Properties of 304 Stainless Steel*

Variation of properties with temperature	Density (kg/m <sup>3</sup> ) * 10 <sup>3</sup>	Poisson's Ratio	Modulus of Elasticity (Pa) * 10 <sup>11</sup>	Yield Strength (Pa) * 10 <sup>8</sup>
0 °C	7.9	0.295	2.0	2.7
200 °C	7.78	0.3	1.9	1.9
400 °C	7.67	0.31	1.8	1.6
600 °C	7.55	0.315	1.7	1.2
800 °C	7.43	0.32	1.5	0.8
1000 °C	7.32	0.327	1.0	0.6
1200 °C	7.2	0.335	0.4	0.55
1400 °C	7.12	0.341	0.5	0.5
1600 °C	7.04	0.346	0.5	0.5

### 2. 1020 Mild Steel

The mechanical properties of 1020 mild steel that have been used in this analysis have been given in table 5.

Table 5: *Mechanical Properties of 1020 mild steel*

Variation of properties with temperature	Density (kg/m <sup>3</sup> ) * 10 <sup>3</sup>	Poisson's Ratio	Modulus of Elasticity (Pa) * 10 <sup>11</sup>	Yield Strength (Pa) * 10 <sup>8</sup>
0 °C	7.8	2.9	2.0	3.1
200 °C	7.8	2.9	1.8	2.5
400 °C	7.8	2.9	1.6	1.8
600 °C	7.8	2.9	1.4	1.1
800 °C	7.8	2.9	0.7	0.4

<b>1000 °C</b>	7.8	2.9	0.6	0.1
<b>1200 °C</b>	7.8	2.9	0.54	0.1
<b>1400 °C</b>	7.8	2.91	0.51	0.1
<b>1600 °C</b>	7.8	2.93	0.49	0.1

### 3. Inconel 625

The mechanical properties of Inconel 625 that have been used in this analysis have been given in table 6.

Table 6: *Mechanical Properties of Inconel 625*

<b>Variation of properties with temperature</b>	<b>Density (kg/m<sup>3</sup>) * 10<sup>3</sup></b>	<b>Poisson's Ratio</b>	<b>Modulus of Elasticity (Pa) * 10<sup>11</sup></b>	<b>Yield Strength (Pa) * 10<sup>8</sup></b>
<b>0 °C</b>	8.51	0.28	2.01	4.64
<b>200 °C</b>	8.498	0.286	1.99	4.29
<b>400 °C</b>	8.487	0.29	1.91	4.10
<b>600 °C</b>	8.475	0.295	1.84	4.08
<b>800 °C</b>	8.463	0.305	1.76	4.05
<b>1000 °C</b>	8.452	0.321	1.68	3.93
<b>1200 °C</b>	8.44	0.34	1.57	3.81
<b>1400 °C</b>	8.429	0.359	1.46	3.7
<b>1600 °C</b>	8.417	0.386	1.38	3.59

#### 3.1.3. Thermal Properties

The thermal properties of the materials that were necessary for this analysis were melting point, thermal conductivity, specific heat and co-efficient of thermal expansion.

##### 1. 304 Stainless Steel

The thermal properties of 304 stainless steel that have been used in this analysis have been given in table 7. The melting point of 304 stainless steel is taken as 1427°C.

Table 7: *Thermal Properties of 304 Stainless Steel*

<b>Variation of properties with temperature</b>	<b>Thermal Conductivity (W/m<sup>0</sup>C)</b>	<b>Specific Heat (J/Kg<sup>0</sup>C)</b>	<b>Thermal Expansion Coefficient (°C<sup>-1</sup>) * 10<sup>-5</sup></b>
<b>0 °C</b>	15	501	1.8
<b>200 °C</b>	18	530	1.9
<b>400 °C</b>	21	580	2.0
<b>600 °C</b>	26	620	2.05
<b>800 °C</b>	34	650	2.1
<b>1000 °C</b>	36	680	2.15
<b>1200 °C</b>	36	690	2.2
<b>1400 °C</b>	36.1	700	2.25
<b>1600 °C</b>	36.1	705	2.29

## 2. 1020 Mild Steel

The thermal properties of 1020mild steel that have been used in this analysis have been given in table 8. The melting point of 1020 Mild Steel has been taken as 1515<sup>0</sup>C.

Table 8: *Thermal Properties of 1020 Mild Steel*

<b>Variation of properties with temperature</b>	<b>Thermal Conductivity (W/m<sup>0</sup>C)</b>	<b>Specific Heat (J/Kg<sup>0</sup>C)</b>	<b>Thermal Expansion Coefficient (°C<sup>-1</sup>) * 10<sup>-5</sup></b>
<b>0 °C</b>	48	480	1.2
<b>200 °C</b>	32	510	1.3
<b>400 °C</b>	30	550	1.3
<b>600 °C</b>	29	600	1.3
<b>800 °C</b>	29	640	1.2
<b>1000 °C</b>	29	680	1.2
<b>1200 °C</b>	30	690	1.2

<b>1400 °C</b>	30	695	1.19
<b>1600 °C</b>	31	702	1.18

### 3. Inconel 625

The thermal properties of Inconel that have been used in this analysis have been given in table 9. The melting point of Inconel 625 is taken as 1404°C.

Table 9: *Thermal Properties of Inconel 625*

<b>Variation of properties with temperature</b>	<b>Thermal Conductivity (W/m°C)</b>	<b>Specific Heat (J/Kg°C)</b>	<b>Thermal Expansion Coefficient (°C<sup>-1</sup>) * 10<sup>-5</sup></b>
<b>0 °C</b>	12.5	456	1.31
<b>200 °C</b>	15.4	501	1.35
<b>400 °C</b>	18.2	552	1.39
<b>600 °C</b>	20.1	597	1.44
<b>800 °C</b>	23.1	649	1.51
<b>1000 °C</b>	26.8	682	1.57
<b>1200 °C</b>	29.4	707	1.66
<b>1400 °C</b>	31.2	718	1.74
<b>1600 °C</b>	32.1	725	1.81

For cooling of the parts after the welding is over the convective heat transfer co-efficient has been taken as 15 W/m<sup>2</sup> °C. The ambient air temperature has been taken equal to 27 °C.

### 3.2. Finite Element Analysis

Finite element analysis has been done in the case of this welding to predict stresses, susceptibility to stress corrosion cracking and the location where failure is most likely to occur. Some of the other methods of analysis were not used due to the following given reasons:

1. Accurate measurement of stresses is very difficult using conventional testing techniques.
2. X-ray method can be used for analysis but it is capable of giving only surface stresses.

3. Neutron Diffraction Method can give the through thickness stress but not the stress distribution.

So, this is the reason why finite element analysis has been used because it is capable of predicting highest risk zone and the stress distribution throughout the parent metals, heat affected zone and the weld metal.

### 3.3. Problem Statement

The problems which have been analysed in this research are three. First aspect is reduction in stresses developed, second is minimization of carbon migration and the third is decreasing the susceptibility to Stress Corrosion Cracking. Considering the above objectives two metal plates, equal in size with a dimension of 300 x 150 x 8 mm are butt welded with filler between them. The parent metal plates are of 304 stainless steel and 1020 mild steel material. The welding arrangement has been shown in Fig 5.

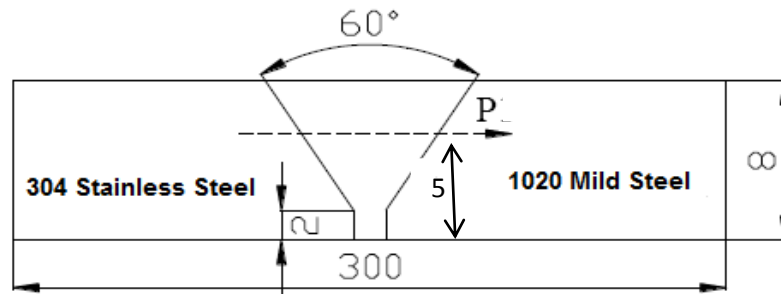


Fig. 5: Schematic representation of the welded joint

The welding simulation has been done firstly by studying the welding temperature field followed by incrementally applying the temperature results to simulate the weld. After the welding process is over residual stresses get developed inside the welded parts. This welded part when kept under operating conditions which are taken as high as 600 °C, results in development of thermal stresses inside the welded part.

The analysis has been done considering three models. Model A is analysed only for thermal stresses and the results are inferred. Model B is analysed only for residual stresses and the results are inferred. Model C is analysed for thermal stresses superimposed with residual stresses. That means mathematically-

$$\text{Model A} + \text{Model B} = \text{Model C}$$

And all the results are taken along the line of length 30mm which lies 5mm above the weld root. Now in the second case, the weld metal A302 Stainless Steel is changed to Inconel 625 and then again the thermal, residual and thermal stress superimposed on residual stresses are calculated.

### 3.4. Assumptions and Conditions

1. Heat flow inside the welded parts is assumed to be by conduction using the fundamental equation of conduction as given in equation (i);

$$k \left( \frac{\partial^2 T}{\partial x^2} + \frac{\partial^2 T}{\partial y^2} + \frac{\partial^2 T}{\partial z^2} \right) + Q_{int} = \rho c \frac{\partial T}{\partial t} \quad (i)$$

, where k is the thermal conductivity, T is the transient temperature field which is a function of time t and Cartesian co-ordinates (x, y, z) with Q as internal heat source rate, ρ as density and c as specific heat capacity.

2. Heat loss from the welded part to the ambient air is assumed to occur by convection following the governing equation of cooling(ii);

$$Q_c = -hA(T_s - T_a) \quad (ii)$$

, where  $Q_c$  is the rate of cooling, h is the convection co-efficient taken here 15 W/m<sup>2</sup> °C for all the cases,  $T_s$  is the surface temperature and  $T_a$  is the temperature of ambient air taken 27 °C.

3. Thermal stress is calculated from the start up at 27 °C to 600 °C. Thermal stress simulated in the welding using its global modelling matrix reduced to give thermal stress at any two nodes is given in equation (iii);

$$\begin{bmatrix} -E\alpha T \\ -E\alpha T \\ 0 \end{bmatrix} = \frac{AE}{L} \begin{bmatrix} 1 & -1 & 0 \\ 0 & 1 & -1 \\ 0 & 0 & 0 \end{bmatrix} \begin{bmatrix} d_1 \\ d_2 \\ d_3 \end{bmatrix} \quad (iii)$$

, where E is the Young's Modulus of Elasticity, T is the transient temperature field, α is the co-efficient of thermal expansion, A is the cross sectional area, L is the length of the section and (d<sub>1</sub>, d<sub>2</sub>, d<sub>3</sub>) are the nodal displacements caused due to temperature load at any three nodes.

However displacement boundary condition d<sub>1</sub>=0 is taken to avoid rank deficiency. In this case of modelling the welded part is assumed to be fixed normal to the weld.

4. For residual stress analysis the elements are activated and deactivated by element birth and death technique. This means that after a weld pass is over on an element, after solidification the element gets structurally activated.

The material properties are set to zero for the deactivated elements. The welding has been carried out at 1500 °C. Therefore, the initial condition for an element after reactivation is its melting point. When an element gets reactivated i.e. born then its mass, element load, etc. are set to their original values.

## Chapter 4

### Results and Discussion

The results that are obtained after the weld simulation can be taken considering two cases. In the first case 302 stainless steel has been taken as the weld filler metal whose properties are taken the same as 304 stainless steel which is one of the parent metals. So the results inferred from all the three models viz. A, B and C which will be taken one by one.

#### 4.1. Case I

##### 302 Stainless Steel as Weld Filler Metal

Thermal stress has developed inside the welded part as both of its ends across the weld have been fixed against any kind of motion by setting up in nodal displacement in all directions as zero. This is the boundary conditions used in model A and model C.

Considering Model A, where only the part has been subjected to thermal stresses the results are explained in the figures below. The figures below show the stress contour near the weld metal and the graphs which are path results along the line of length 30 mm at the centre of the filler metal and at a distance of 5 mm from the weld root. The line is called line P in the subsequent paragraphs.

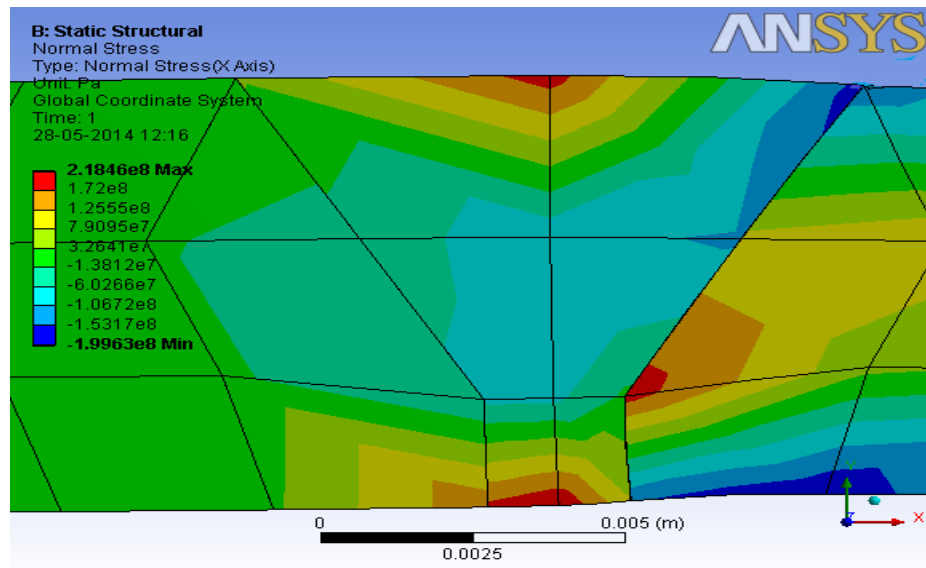


Fig. 6: Normal stress contour of Model A

The normal stress varies from 218 MPa tensile to 199 MPa compressive. The peak of the tensile lies along the centreline of the weld metal. However peak of the compressive stress lies in the weld interface of weld filler metal and 1020 mild steel.



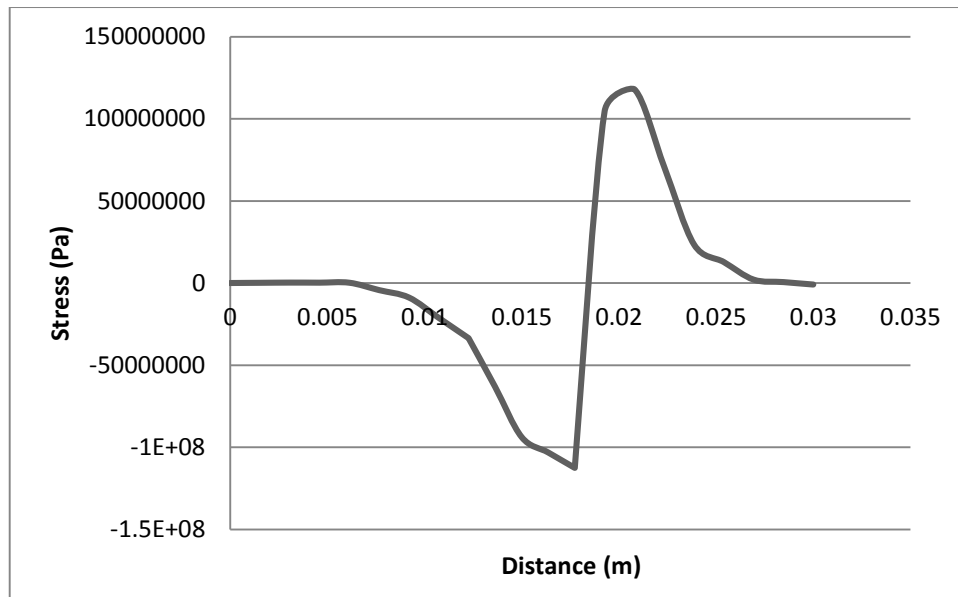


Fig. 7: Normal stress distribution along line P

The normal stress along the line P in both directions is found in the weld interface near the 1020 mild steel. The maximum stress is found to be 118 MPa in the tensile direction.

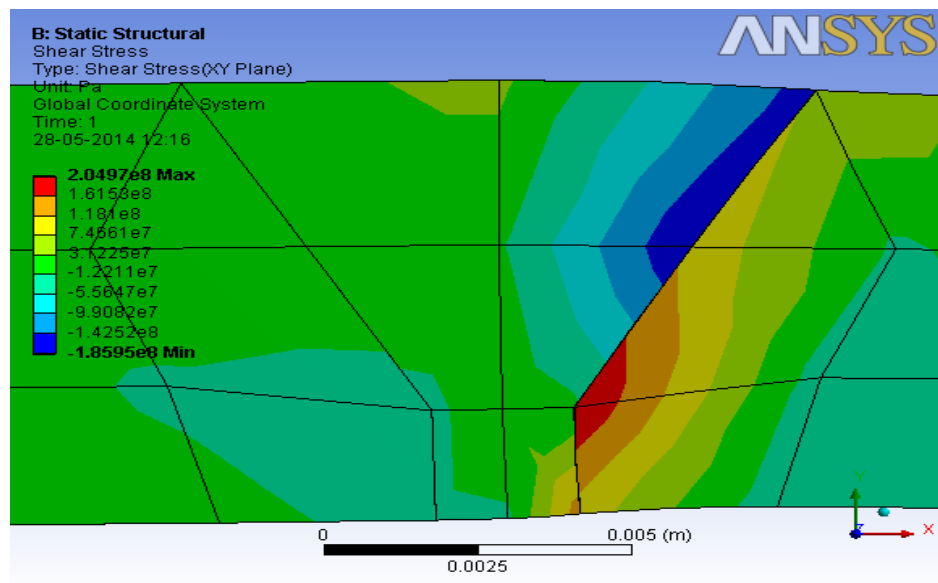


Fig. 8: Shear stress contour of Model A

The shear stress varies from 204 MPa positive to 186 MPa negative. However peak of the shear stress lies in the weld interface of weld filler metal and 1020 mild steel. From the above two cases it is very clear that the weld interface on the 1020 mild steel is the highest risk zone, where the failure is most likely to occur. The shear stress distribution along the line P is shown in Fig. 9.

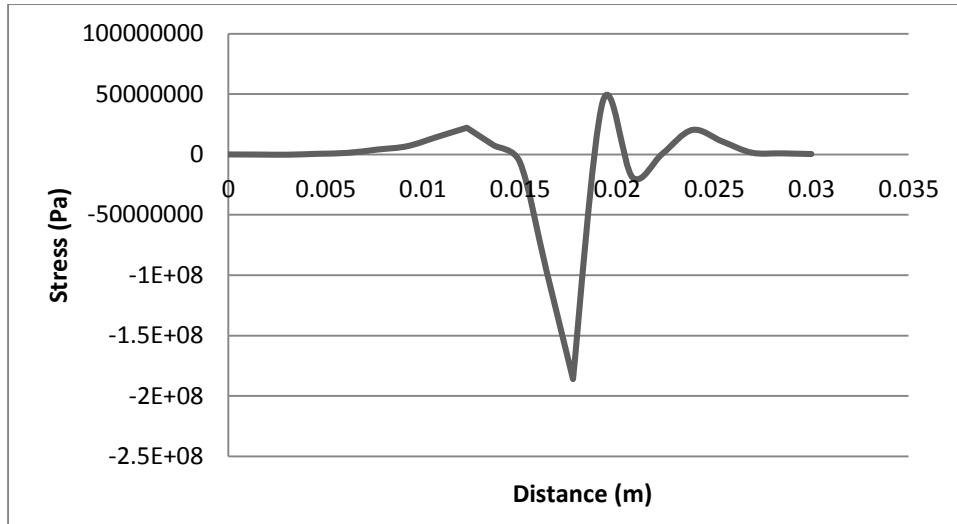


Fig. 9: *Shear stress distribution along line P*

The maximum shear stress along the line P is 186 MPa along the negative direction and also is located in the weld interface on 1020 mild steel side.

Now taking up the case where residual stresses have developed as a result of heating and subsequent cooling during the welding process.

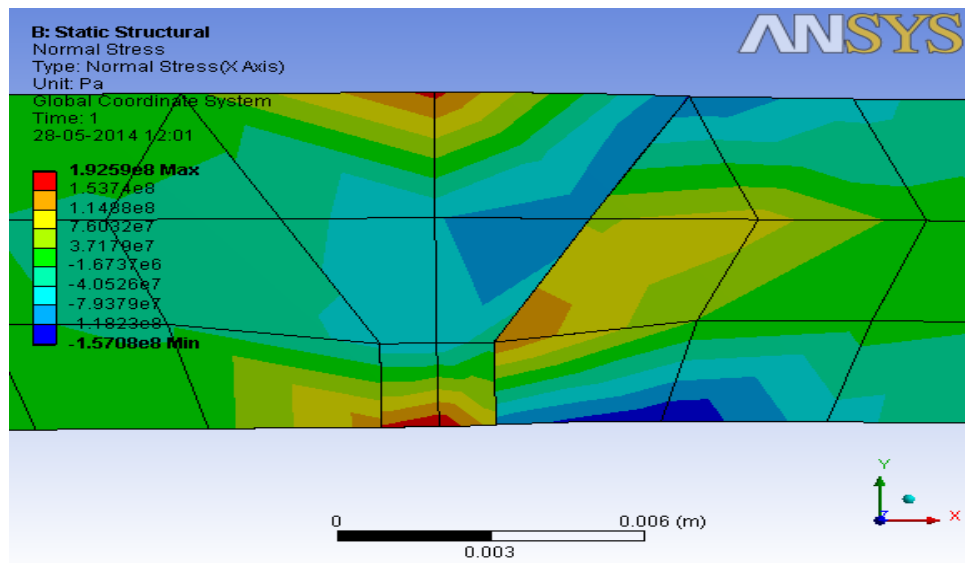


Fig. 10: *Normal stress contour of Model B*

The normal stress varies from 192 MPa tensile to 157 MPa compressive. The peak of the tensile lies on the 1020 mild steel and compressive stress lies in the 304 stainless steel side. This is due to larger coefficient of thermal expansion of 304 stainless steel. The stress gradient in the filler metal is very steep due to rapid change in the direction of stresses.

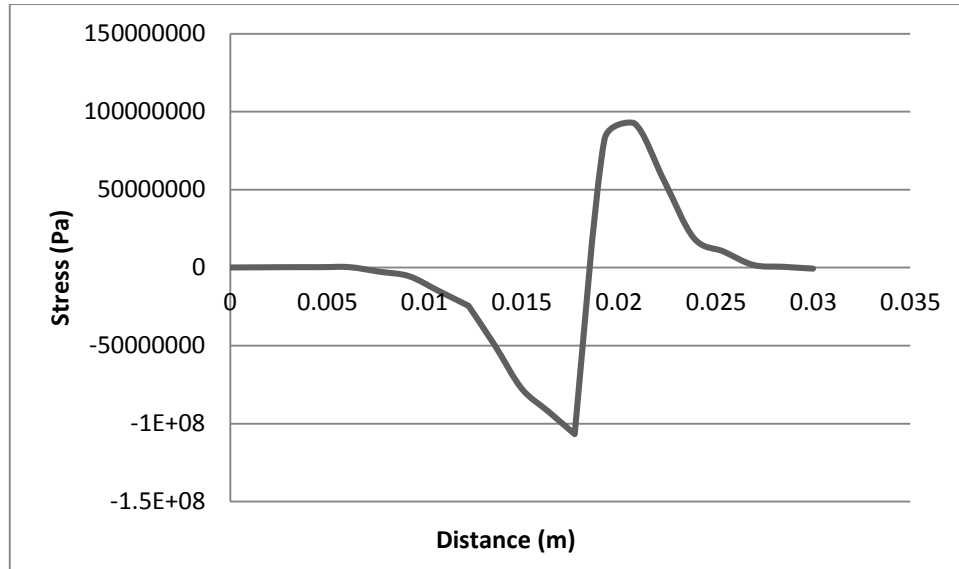


Fig. 11: Normal stress distribution along line P

The maximum stress is induced in the weld interface on the 1020 mild steel side and its magnitude is 107 MPa and is of compressive nature. The steep gradient in the stress in this zone represents the vulnerability of this zone to cracking.

Similarly the shear stress contour in the XY-plane developed in the model B is shown in the Fig. 12.

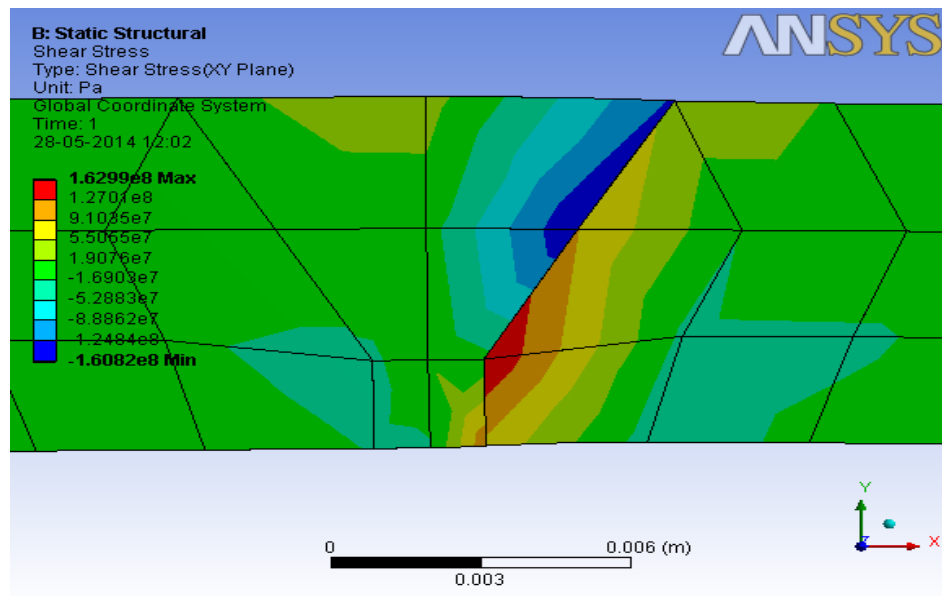


Fig. 12: Shear stress contour of Model B

The shear stress varies from 204 MPa positive to 186 MPa negative. However peak of the shear stress lies in the weld interface of weld filler metal and 1020 mild steel. The extremes of stress in both directions also lie in the same location making it the weakest part.

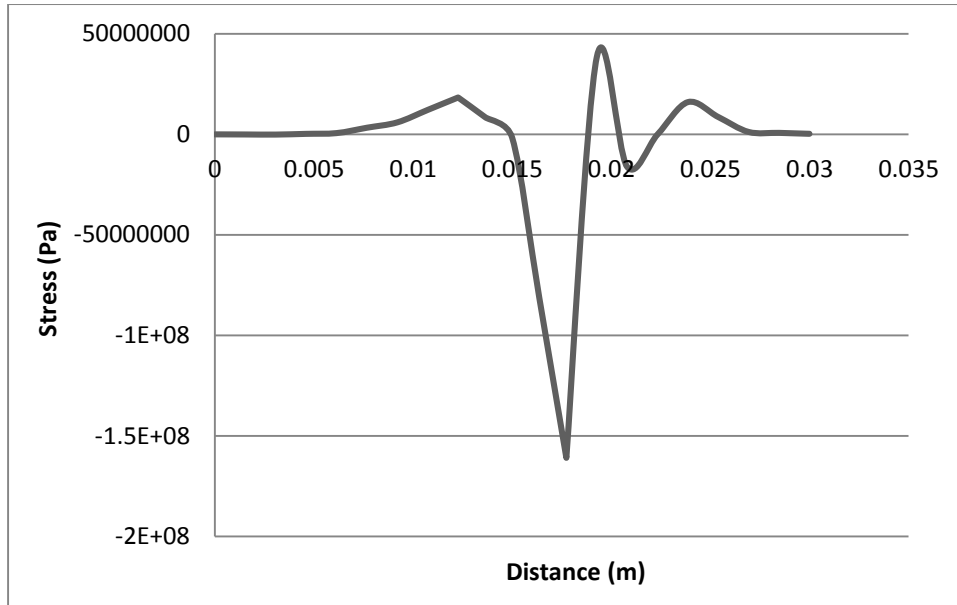


Fig. 13: *Shear stress distribution along line P*

The maximum value of shear stress along the line P is found to be 161 MPa, and the stress is in clockwise direction which is assumed to be negative direction. At the weld interface on 1020 mild steel side, shear stress rises falls very rapidly.

In the model C, where the thermal stress is superimposed on residual stress the normal stress contour developed is shown in Fig. 14.

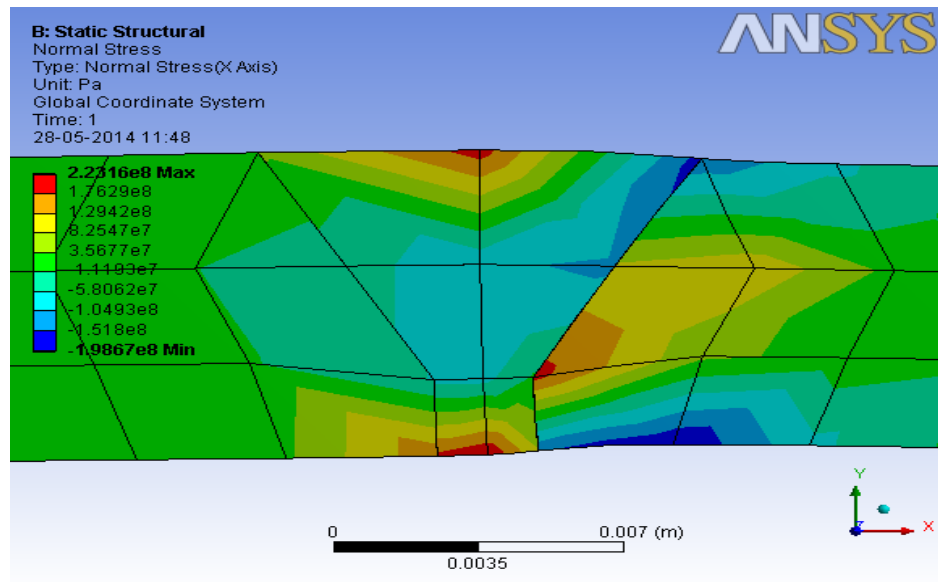


Fig. 14: *Normal stress contour of Model C*

The value of normal stresses developed in the welded joint in the model C is 223 MPa of the tensile nature and 198 MPa of the compressive nature. The maximum tensile stress is located at the centre of the welded joint and is much localised.

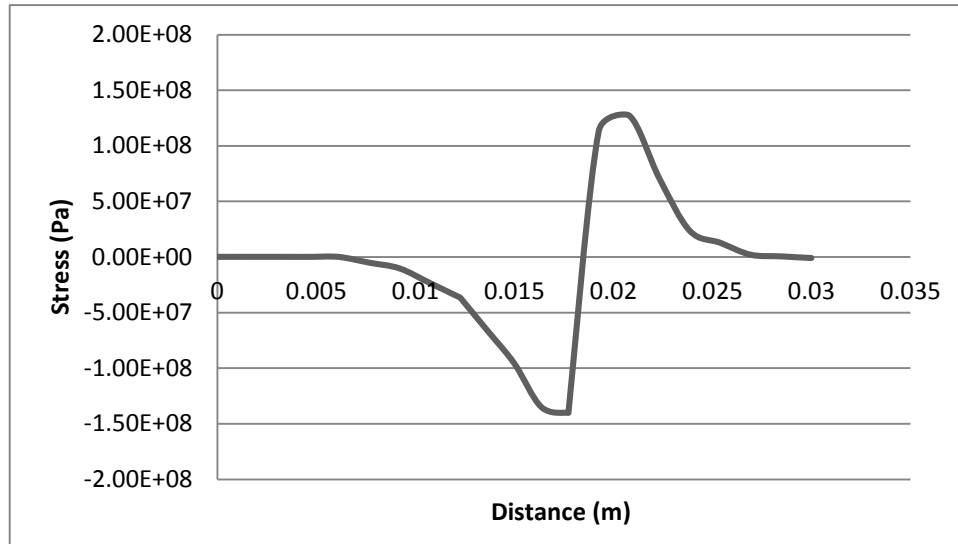


Fig. 15: Normal stress distribution along line P

The stress distribution graph that normal stress value is highest i.e. 140 MPa near the weld interface on the 1020 mild steel side. The magnitude of stress is highest in both the directions at this very location.

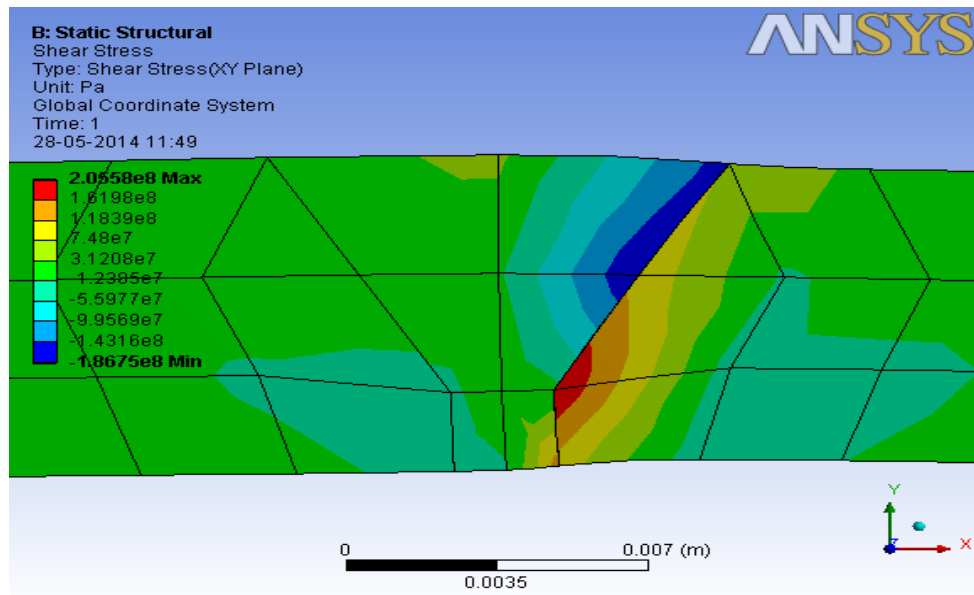


Fig. 16: Shear stress contour of Model C

Similarly the shear stress contour in XY-plane as shown in Fig. 16 indicates a high cyclic reversal of stresses at the weld interface on 1020 mild steel side. The value of stress here varies from 205 MPa counter-clockwise to 186 MPa in the clockwise sense. By the virtue of shear stress developed it is quite clear that the welded joint is most likely to break at the weld interface on 1020 mild steel side.

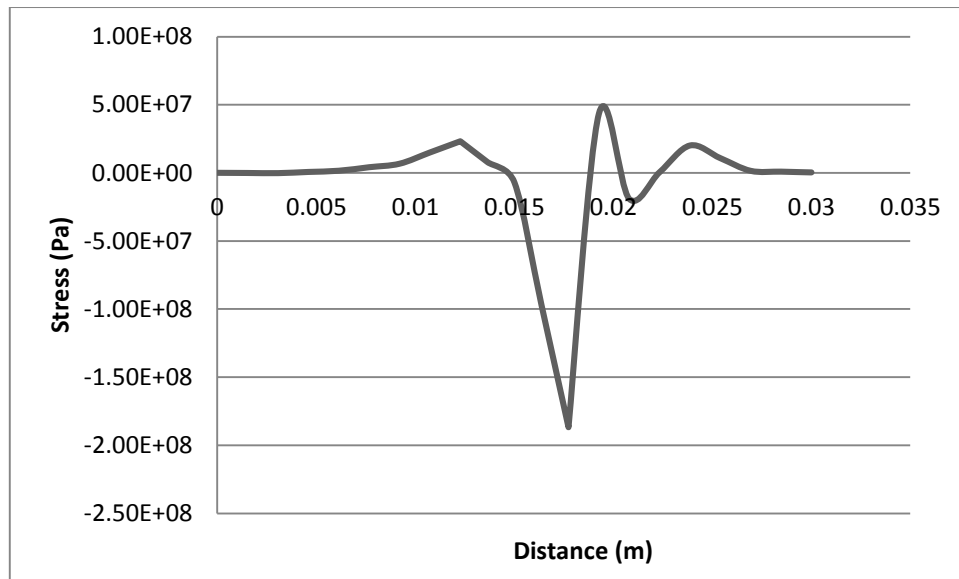


Fig. 17: *Shear stress distribution along line P*

The path results obtained on the line P also confirm that there is a huge cyclic reversal of stresses in the zone mentioned above. The maximum value of shear stress i.e. 187 MPa is also present on this particular line.

The analysis of strain which is a parameter in deciding the susceptibility of stress corrosion cracking is discussed in the next paragraph.

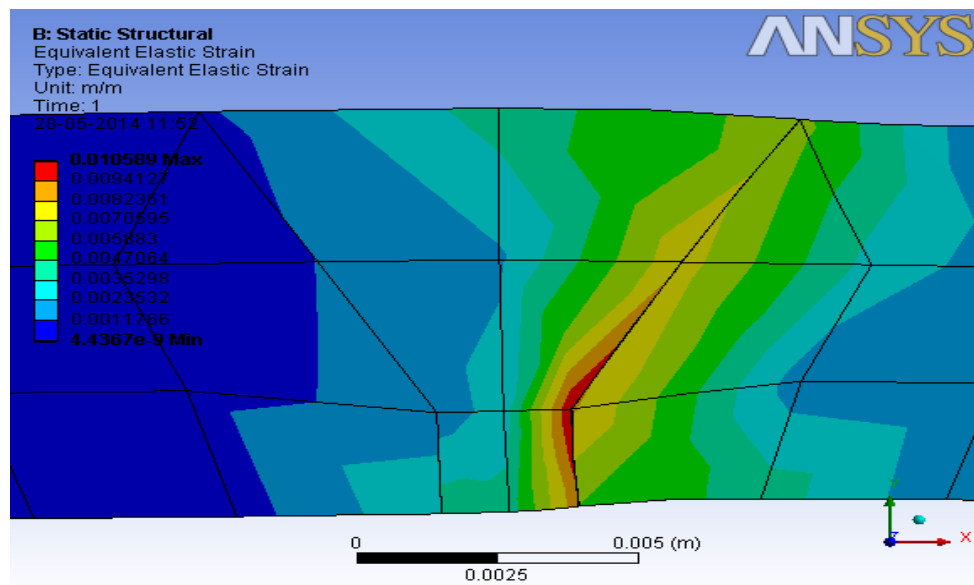


Fig 18: *Equivalent strain contour in Model C*

In line with the stresses the contour of equivalent strain also depicts that a maximum strain of 0.01 m/m is also located in the weld interface on the 1020 mild steel side. This means that this interface has the highest deformation.

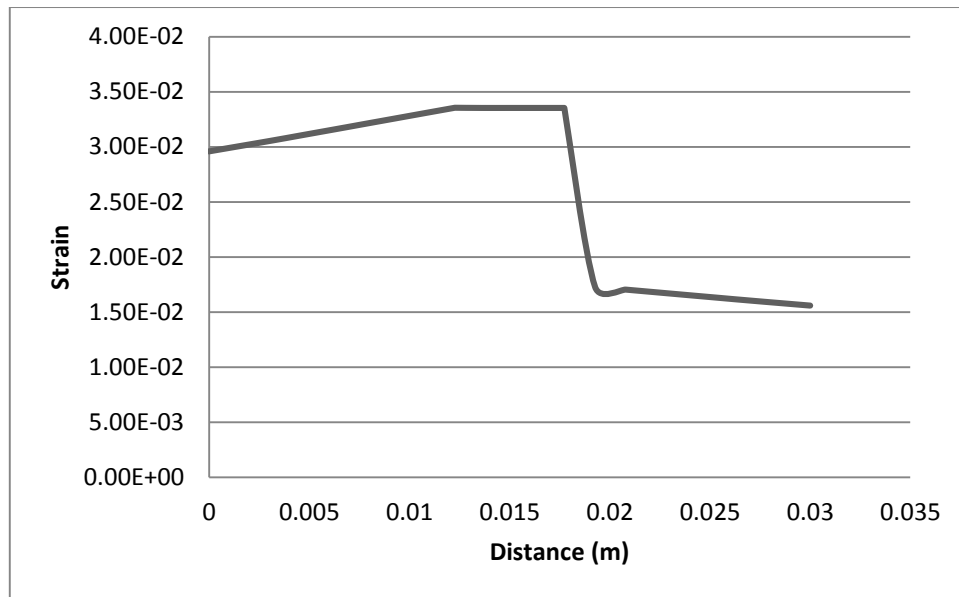


Fig 19: *Equivalent strain distribution along the line P*

The value of maximum equivalent strain is 0.0335 m/m and its value remain almost constant in the HAZ of 304 stainless steel and reach its peak in the weld metal zone and then recede rapidly in the 1020 mild steel side.

Having seen these problems of high stress and strain with 302 stainless steel as the weld metal, Inconel 625 replaces it for the next analysis.

## 4.2. Case II

### Inconel 625 as Weld Filler Metal

Now the weld metal is changed from 302 stainless steel to Inconel 625. Inconel 625 has been chosen because of its material properties, which are intermediate between 304 stainless steel and 1020 mild steel. Again the welded joint is simulated as in case I, keeping all the other boundary condition same.

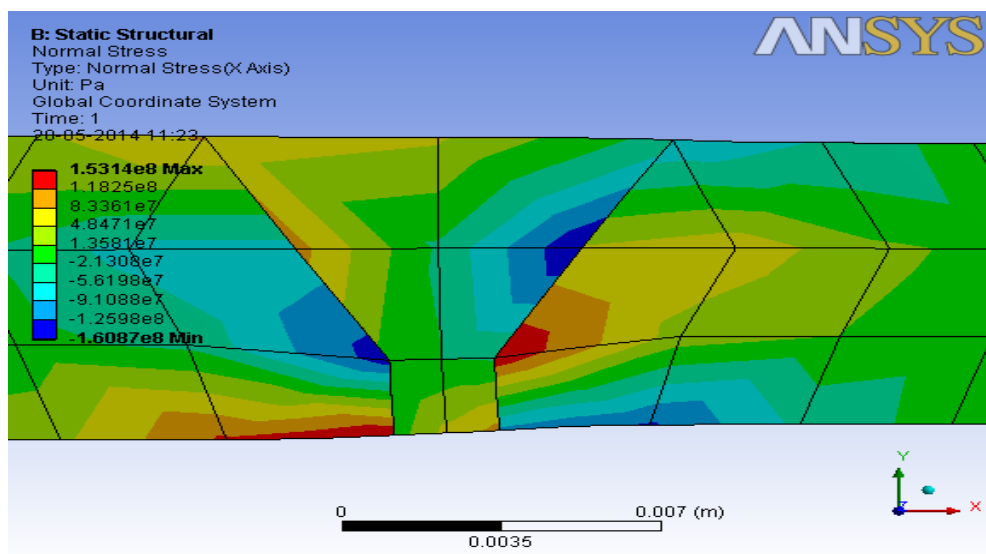


Fig. 20: *Normal stress contour of Model A*

The value of stress varies from 153 MPa tensile to 160 MPa compressive. A notable change that can be observed from the previous case is that the rise in stress is not limited only in 1020 stainless steel side but a somewhat lower but appreciable rise is also seen in the 304 stainless steel side.

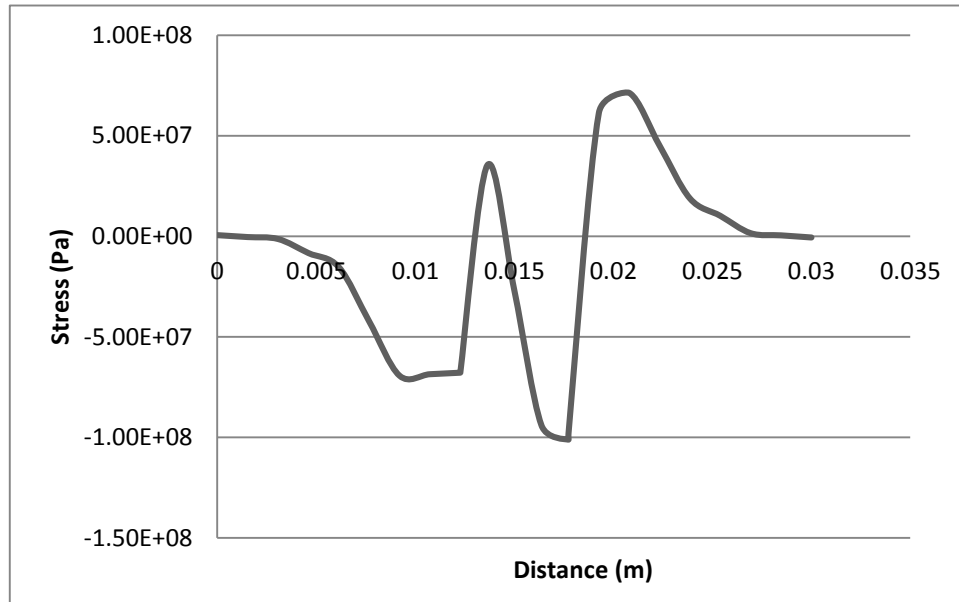


Fig 21: Normal Stress distribution along line P

The values of maximum stress on 304 stainless steel side is 71 MPa and while a maximum of 101 MPa is found on 1020 mild steel side.

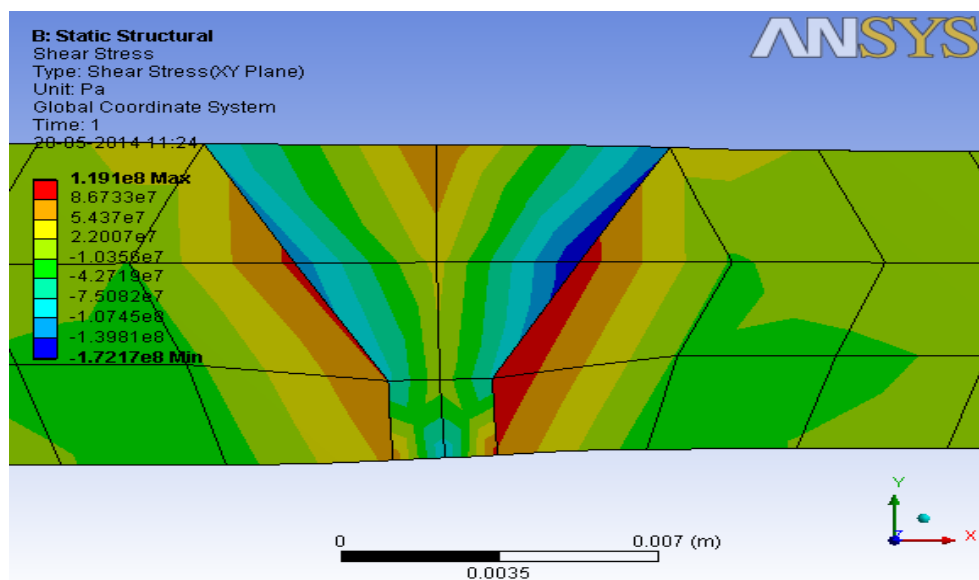


Fig. 22: Shear stress contour of Model A

Shear stress values in the XY-plane vary from 119 MPa counter-clockwise to 172 MPa in the clockwise sense. It is to be noted that high cyclic shear stresses have developed in the weld interface on 1020 mild steel side and in terms of shear stress this side of weld metal is still the highest risk zone.



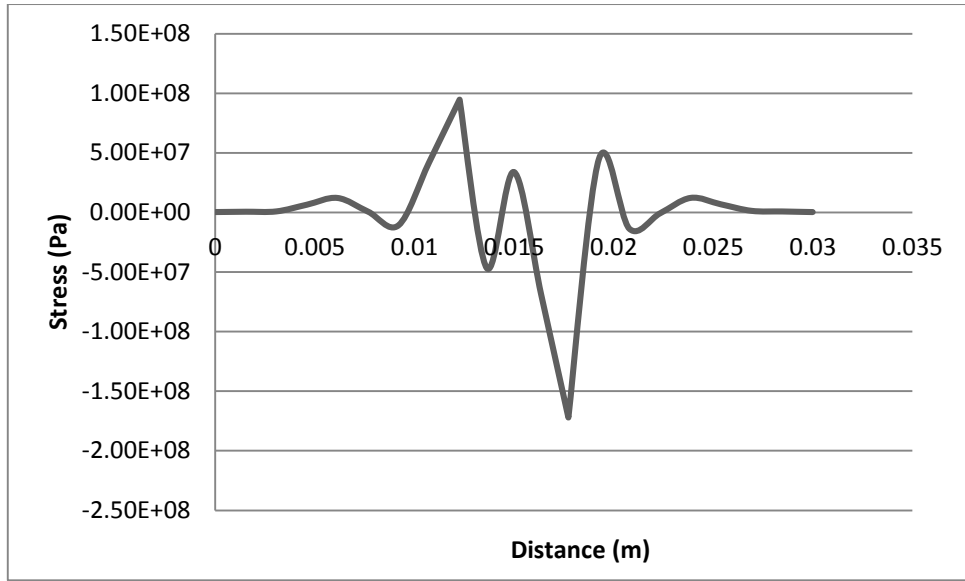


Fig 23: Shear stress distribution along line P

The maximum value of shear stress which is 172 MPa falls on the line P, which depicts that the weakest point falls at a distance of 5 mm from the weld root near the 1020 mild steel side.

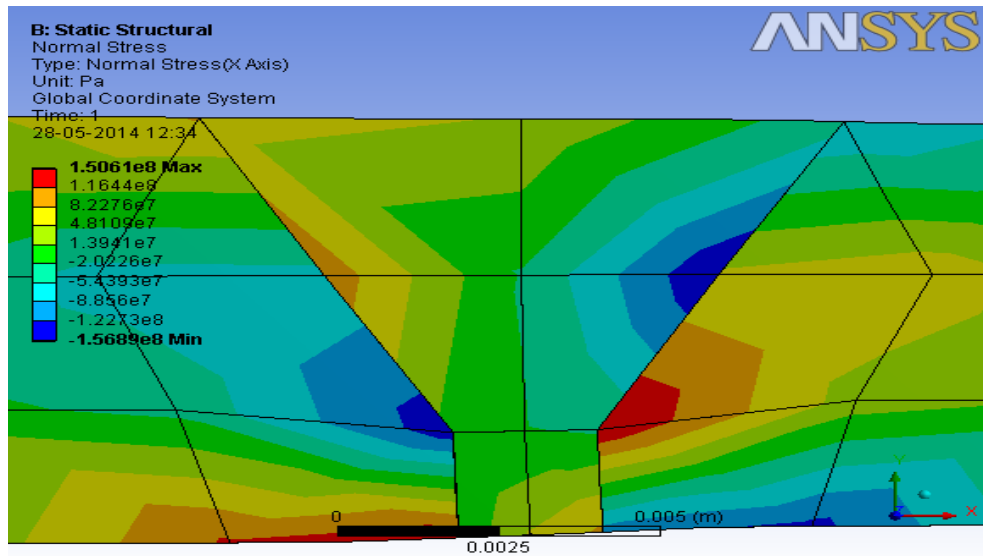


Fig. 24: Normal stress contour of Model B

For the case wherein residual stress has developed due to cooling after welding the value of stress varies from 150 MPa in tensile sense to 156 MPa in the compressive sense.

As shown in the contour diagram tensile stresses have developed on 1020 side while 304 stainless steel and Inconel have compressive stress developed in their region.

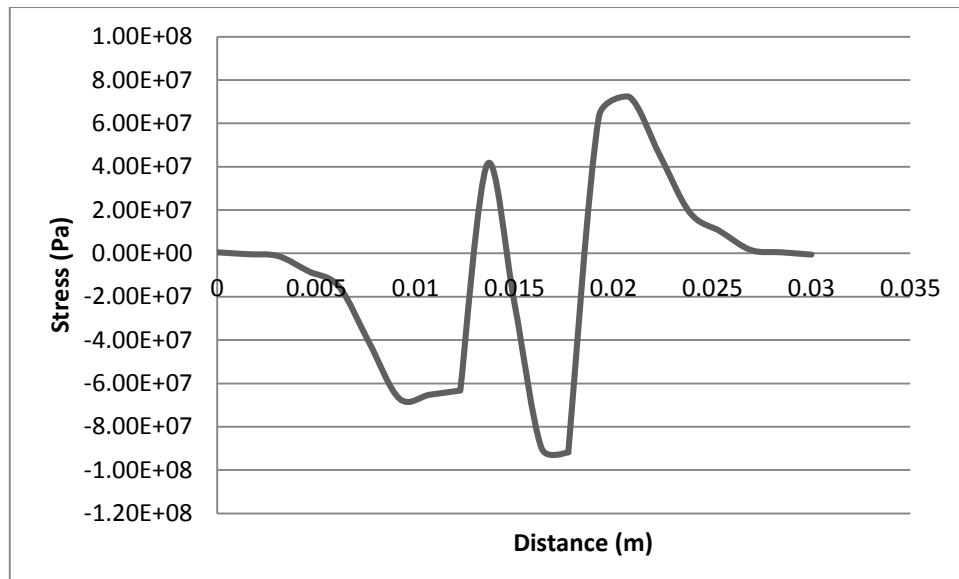


Fig 25: Normal stress distribution along line P

The maximum value of normal stress is found in the weld interface near the 1020 mild steel and its value is 91 MPa which is compressive in nature. However the value of stress in terms of magnitude is found to be uniformly increasing and decreasing along the weld metal.

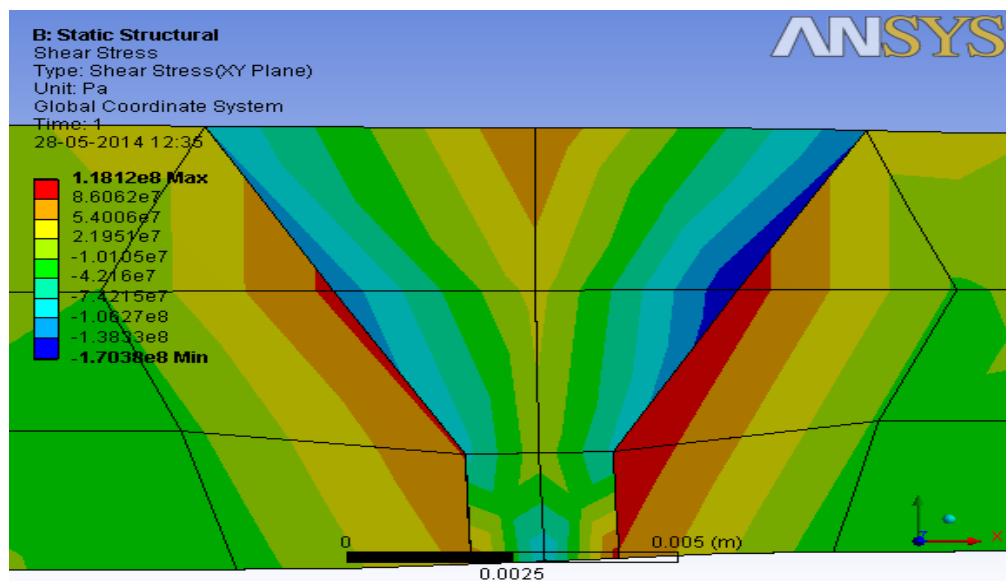


Fig. 26: Shear stress contour of Model B

The shear stress developed in the welded part in XY-plane is 118 MPa in the counter-clockwise sense and 170 MPa in the clockwise sense. Both the peaks of clockwise and counter-clockwise are present on the weld interface on the 1020 mild steel side.

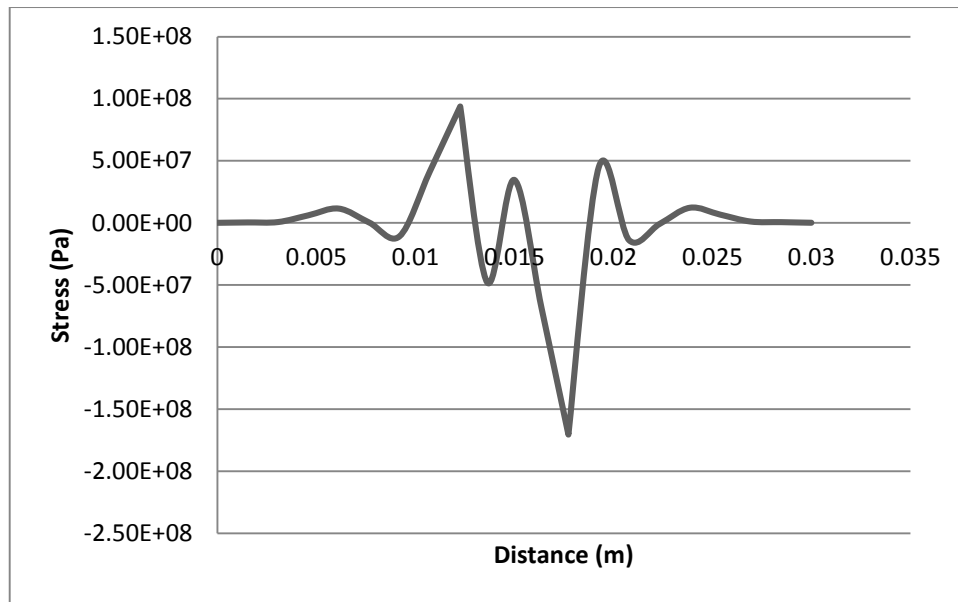


Fig. 27: Shear stress distribution along line P

The variation in shear stress along the weld metal is very rapidly changing in a cyclic fashion. The value of maximum shear stress in clockwise sense is located at the weld interface on 1020 mild steel side on the line P and its value is 170 MPa.

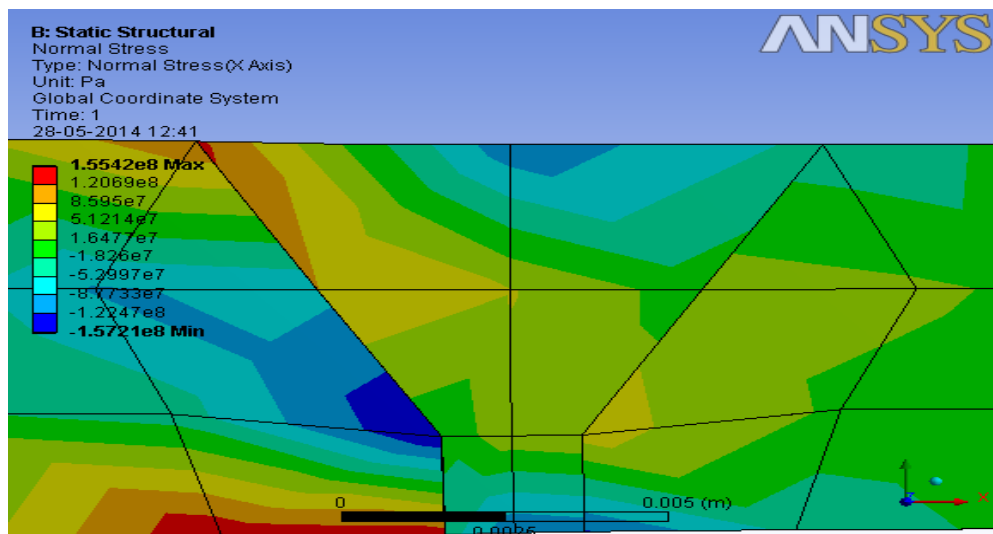


Fig. 28: Normal stress contour of Model C

The model C which is superimposed thermal stress on residual stress the maximum normal stress has shifted away from the weld metal zone towards the side of 304 stainless steel.

Even if the highest value of stress is about 155 MPa tensile and 157 MPa compressive, but still the value of normal stress in the weld metal zone is very low as depicted by Fig. 29.

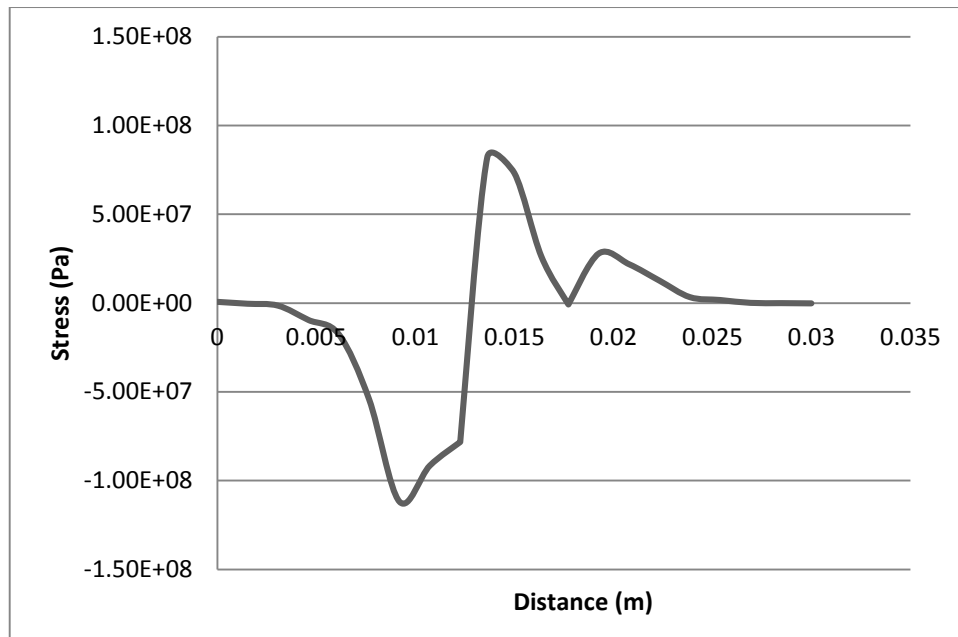


Fig. 29: Normal stress distribution along line P

Fig. 29 shows the value of maximum normal stress of around 102 MPa along the line P, which is almost half of the maximum stress developed in the entire welded part. Almost entire of the weld zone has nearly equal value of stress as shown in Fig. 28. This is the advantage by using Inconel 625 as a weld metal which reduces the stress developed in the weld metal zone and makes the joint safer.

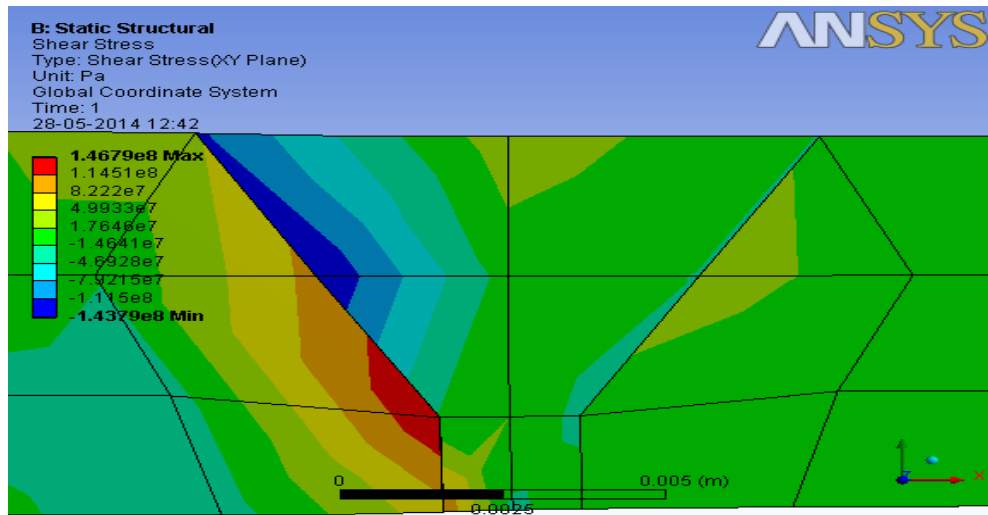


Fig. 30: Shear stress contour of Model C

The value of the shear stress in the XY-plane developed is highest in the weld interface on the 304 stainless steel side. The value of the stress varies from 146 MPa in counter-clockwise sense and 143 MPa in clockwise sense. Even if the highest stress has changed places between the interfaces, but still its value has decreased.

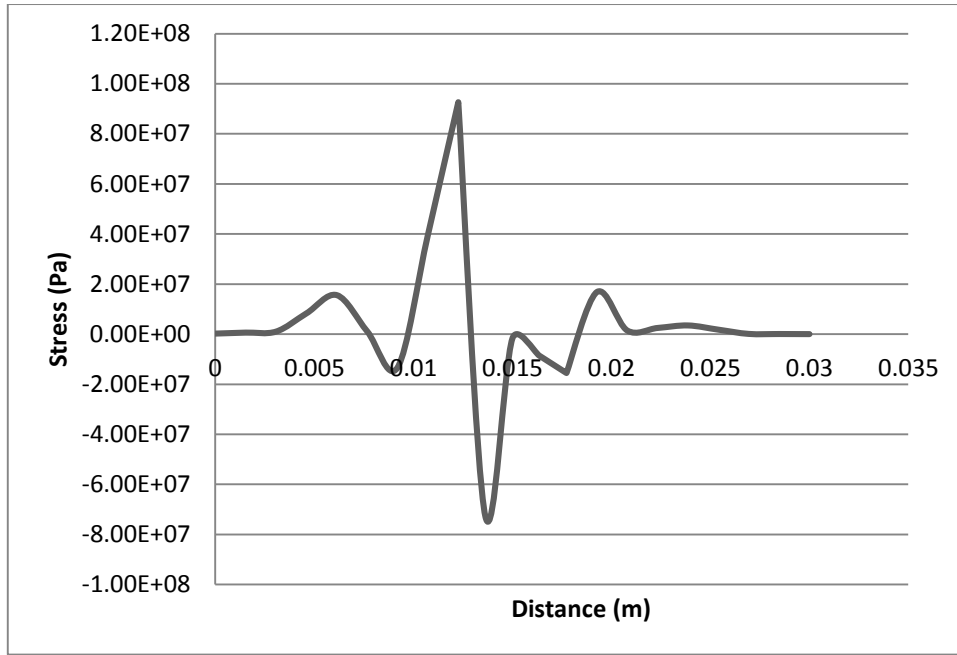


Fig. 31: *Shear stress distribution along line P*

The same is depicted by Fig. 31, as the highest value of stress along the line P is found to be 92.6 MPa. The cyclic variation of stress is near the 304 stainless steel side but still the value of stress is appreciably lower than that in case of 302 stainless steel as the weld metal.

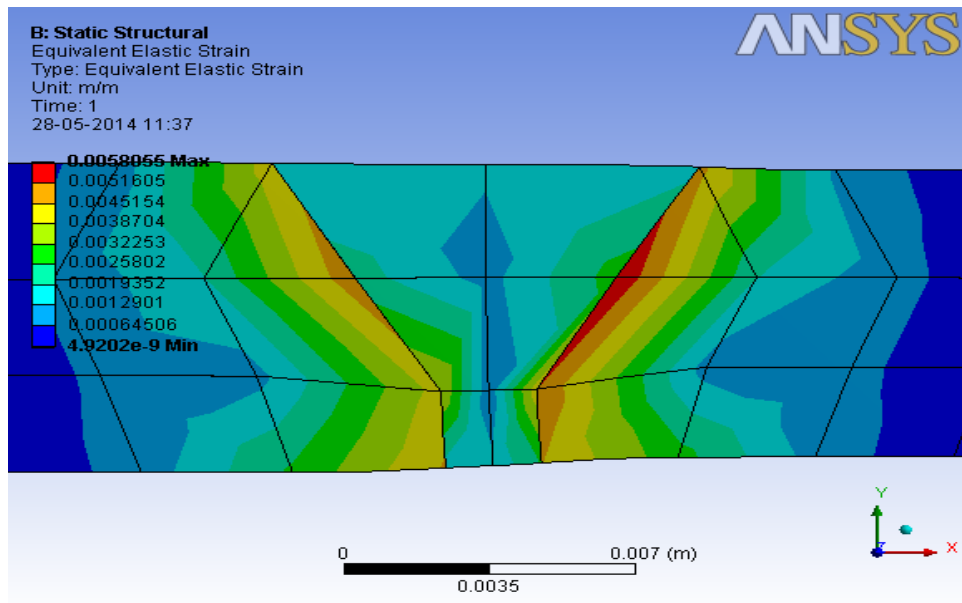


Fig. 32: *Equivalent strain contour for Model C*

Now, finally considering the strain developed in the model C, it is found that the value of equivalent strain varies from 0.0058 to a minimum of  $4.92 \times 10^{-9}$ . The peak value of strain lies in the weld interface on the 1020 mild steel side. The values of strain are found higher only in the HAZ of parent metals and most of the weld metal has developed negligible strain.

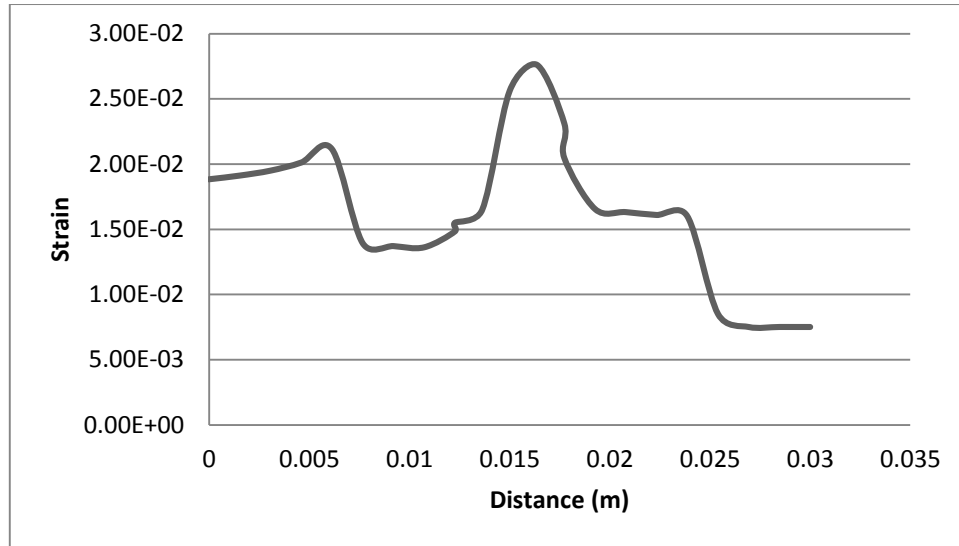


Fig. 33: *Equivalent strain distribution along line P*

The equivalent strain along the line P shows higher values of strain in the heat affected zone of the parent metal and whose values decrease within the weld metal. The peak value of strain along the path is 0.0276 m/m.

After getting the results, the data regarding the maximum values of normal stress along the line P is tabulated comparing both the cases of welding;

Table 10: *Comparison of normal stress values in the two cases of welding*

Models	Nature of Stress	Case I: 302 Stainless Steel	Case II: Inconel 625
A	Tensile	118 MPa	71 MPa
	Compressive	112 MPa	101 MPa
B	Tensile	92 MPa	63 MPa
	Compressive	107 MPa	91 MPa
C	Tensile	127 MPa	82 MPa
	Compressive	140 MPa	112 MPa

From the above table some of the results that can be inferred are mentioned below:

1. The maximum value of superimposed stress i.e. Model C is greater than the maximum values of both the thermal stress and weld residual stress in all the cases.
2. This explains the reason why it is necessary to consider the weld residual stress while exposing a welded part to cyclic thermal stresses. It will be an

underestimation of the maximum working stress and result finally into an unsafe joint.

3. The values of stress both either of compressive or of tensile nature are found to be reduced significantly when the weld metal is changed from 302 stainless steel to Inconel 625.

It is obvious from the stress contour diagrams in the case I the highest values of stresses were in the weld interface on the 1020 mild steel side. Hence it is the weakest location the welded part.

Now from table 1 and table 2 it is clear that the carbon concentration in 1020 mild steel is much higher than that in 304 stainless steel. As a result of which, during welding or any other subsequent high temperature operation carbon atoms will diffuse from 1020 mild steel into the weld metal. So a carbon depleted zone is formed in the HAZ of 1020 mild steel and a carbon enriched zone is formed in the weld metal.

The carbon diffusion will change the material properties and will greatly influence life of the joint [12]. Since the value of stress as shown in the contour diagrams change drastically in this interfacial zone, the resultant stress gradient will accelerate carbon diffusion. [11]

Therefore, carbon diffusion, thermal and residual stress which plays an important role in the service life of a component needs to be reduced. One method of solving this problem is to choose a weld metal having co-efficient of thermal expansion intermediate between 1020 mild steel and 304 stainless steel, and other is to choose a weld metal that can reduce carbon diffusion.

Sireesha et al. [12] suggested that Inconel as a filler material is the best option available in welding dissimilar steels. This is because nickel-based consumable alloys exhibit better tensile strength, resistance to hot cracking and thermal stability compared to steels. Also carbon movement activity is also retarded due to low diffusivity of carbon in nickel-based alloys.

This is the reason why Inconel 625 has been used for welding in the second case and the results obtained have clearly proved the theory behind. Only exception that can be taken is shifting of high stress zone in both the interfaces which was earlier only on the 1020 mild steel side. But the value of these stresses is very low i.e. 15-30% lower than those obtained by using 302 stainless steel as the weld metal.

In dissimilar welding joint, Stress Corrosion Cracking. To appreciate the susceptibility to Stress Corrosion Cracking, hardness is an important factor which goes hand in hand with strain hardening. So the values of strain have also been calculated in this research. [13]

From Fig. 19, the strain developed in the weld metal and the HAZ of parent metals is found to have a maximum value of 0.0335 m/m in the weld metal zone. After Inconel 625 is used as the weld metal, the highest value of strain is reduced to 0.0276 m/m as shown in Fig. 33.

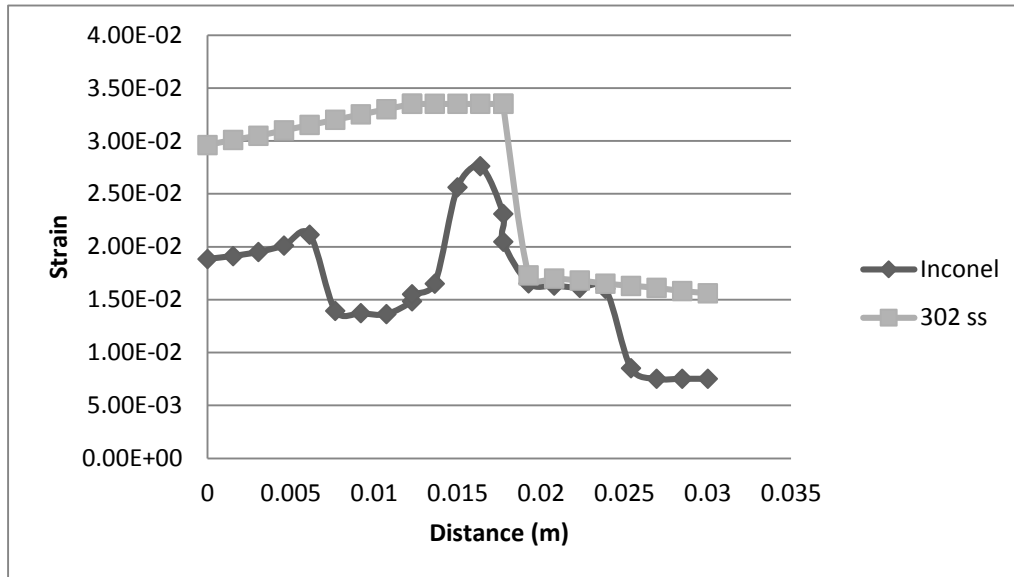


Fig. 34: Comparison of strain values between case I and case II

Fig. 34 shows that the value of strain induced in Inconel weld metal is significantly lower than that induced in 302 stainless steel weld metal throughout the path line P. The reduction in maximum strain is 17%.



## Chapter 5

### Conclusions

This research presents a study of thermal stress in a dissimilar welding joint between 1020 mild steel and 304 stainless steel, and the effect of weld residual stress on the thermal stress has been discussed. From the results above we arrive at the following conclusions:

1. Welding which is a significant cause of residual stress generates a large amount of residual stress in the weld metal and HAZ of the parent metals, which increases the final thermal stress and should be considered while determining the strength of the joint.
2. If the residual stresses are not considered, due to lower co-efficient of thermal expansion, 1020 mild steel develops tensile thermal stress while compressive thermal stress is generated in 304 stainless steel during operating conditions.
3. The peak of the stress is reached in the weld interface of 1020 mild steel and weld metal near the mild steel side, which becomes the highest risk zone.
4. If A302 steel is replaced by Inconel 625 then the developed peak stress falls by 15-30%, and hence the welded joint becomes safer.
5. Inconel 625 is recommended to be used as the weld metal, because it also reduces strain which is an index of stress corrosion cracking as result of which the chances of stress corrosion cracking are reduced by 17%.
6. Also by introducing a weld metal which is a nickel-based alloy decreases the carbon activity gradient due to its low carbon diffusivity. Thus there is no abrupt change in material composition and hence a steep stress gradient is avoided.

A future work that can be undertaken from this research can be:

1. Superimposing fatigue loads on welded parts.
2. Introduction of a new weld metal that can still improve the results than Inconel 625 for dissimilar steels.

## Chapter 6

### References

- [1] Chengwu Yao, Binshi Xu, Xiancheng Zhang, Jian, Huang, Jun Fu and Yixiong Wu “Interface microstructure and mechanical properties of laser welding copper-steel dissimilar joint” *Optics and Lasers in Engineering*, Vol. 47, 2009, PP 807–814.
- [2] Wen-chun Jiang and Xue-wei Guan “A study of the residual stress and deformation in the welding between half-pipe jacket and shell” *Materials and Design*, Vol. 43, 2013, PP 213-219.
- [3] Man Gyun Na, Jin Weon Kim and Dong Hyuk Lim “Prediction of Residual Stress for dissimilar metals welding at nuclear plants using Fuzzy Neural Network Models” *Nuclear Engineering and Technology*, Vol. 39, 2007, PP 337-348.
- [4] M.M.A. Khan, L. Romoli, M. Fiaschi, G. Dini and F. Sarri “Laser beam welding of dissimilar stainless steels in a fillet joint configuration” *Journal of Materials Processing Technology*, Vol. 212, 2012, PP 856-867.
- [5] Yoshiyasu Itoh and Kabushiki Kaisha Toshiba “Joined structure of dissimilar metallic materials” *Patent Publication Number*, EP0923145A2, 1999.
- [6] P. Delphin, I. Sattari-Far and B. Brickstad “Effect of thermal and weld induced residual stresses on the j-integral and ctod in elastic-plastic fracture analyses” *Final Report* Vol. SINTAP/SAQ/03, 1998, PP 1-47.
- [7] T.A. Mai and A.C. Spowage “Characterization of dissimilar joints in laser welding of steel-kovar, copper-steel and copper-aluminium” *Materials Science and Engineering*, Vol. 374, 2004, PP 224-233.
- [8] Paul Colegrove, Chukwugozie Ikeagu, Adam Thistlethwaite, Stewart Williams, Tamas Nagy, Wojciech Suder, Axel Steuwer and Thilo Pirling “The welding process impact on residual stress and distortion” *Science and Technology of Welding and Joining*, Vol. 14, 2009, PP 717-725.
- [9] N. Arunkumar, P. Duraisamy and S. Veeramanikandan “Evaluation Of Mechanical Properties Of Dissimilar Metal Tube Welded Joints Using Inert Gas Welding” *International Journal of Engineering Research and Applications*, Vol. 2, Issue 5, 2012, PP 1709-1717.
- [10] Wei-Chih Chung, Jiunn-Yuan Huang, Leu-Wen Tsay and Chun Chen “Microstructure and Stress Corrosion Cracking Behavior of the Weld Metal in Alloy 52-A508 Dissimilar Welds” *Materials Transactions*, Vol. 52, 2011, PP 12-19.

- [11]C.D. Lundin “Dissimilar Metal Welds” *Welding Research Supplement*, Vol. 62, 1982, PP 58-72.
- [12] Shireesha M, Shaju K Albert, Shankar V, Sundaresan S. “A comparative evaluation of welding consumables for dissimilar welds between 316LN austenitic stainless steel and Alloy 800” *Journal of Nuclear Materials*, Vol. 279, 2000, PP 65-76.
- [13]Li Yongkui, Yoshiyuki Kaji, Takahiro Igarashi “Effects of thermal load and cooling condition on weld residual stress in a core shroud with numerical simulation” *Nuclear Engineering and Design*, Vol. 242, 2012, PP 100-107.